Studies of Quantum Rings with Variational Monte Carlo Method

Liam Sebestyén

September 8, 2016

Contents

Abstract

The variational Monte Carlo method is used to obtain an approximation of the ground state wave function for one and two particles in a quantum dot, one ring and two concentric rings. For the quantum dot, the potential of a harmonic oscillator is used. A shifted harmonic oscillator potential is used to describe the ring. Different trial wave functions are tried and compared for the systems. The energies for one particle in one ring and two concentric rings are compared with results obtained by an existing routine, which uses expansion in B-splines and exact diagonalization, and good agreement are found. For one and two particles in one ring, the effect of the radii is studied. The largest number of parameters in the trial wave function is found to be needed for a small ring to get accurate results. Fewer parameters are needed for a large ring and when the ring is close to a dot. For one particle the energy as a function of radius decreases to a minimum for small radii after which it slowly increases to the energy for one particle in a two dimensional harmonic oscillator. The energy is found to decrease as the radius is increased for two particles in one ring. For large radii the energy approaches twice the value of one particle in a one dimensional harmonic oscillator. For two particles in two rings the probability to be in the inner ring decreases as the outer radius is increased, the opposite of the one particle case.

Chapter 1

Introduction

Quantum rings and dots are nanometre-sized artificial molecules. They are larger than molecules, but still small enough so that quantum mechanics is needed to describe them. These so called nanocrystals can be used as building blocks in microelectronics. One possible application is as storage devices in quantum computers.

Quantum dots and rings are mostly made using heterostructures. Heterostructures are made up of semiconducting materials with different band gaps. When making quantum dots and rings small areas of lower band gap are created in larger areas of higher band gap. One heterostructure used is GaAs/AlGaAs. Nano-lithographic methods on semiconducting surfaces is one way quantum rings have been made [1]. Another way quantum rings have been constructed is with self-assembling InGaAs-rings [2]. In the experiment by Lorke *et al* [2], each ring contained one to two electrons and were 2 nm high, had an outer diameter of 60-140 nm and a well-defined hole with diameter 20 nm.

In this thesis the Variational Quantum Monte Carlo method will be used to obtain an approximation of the ground state wave function for one and two particles in a quantum dot, one ring and two concentric rings. With Quantum Monte Carlo the computational time increases much slower when the number of particles is increased than when using many other methods. A disadvantage of the Variational Monte Carlo is that only the ground state can easily be obtained.

For one particle, the results were compared with the results from an existing routine which uses diagonalization in a B-spline basis.

Chapter 2

Method

2.1 Modelling quantum dots and rings

2.1.1 One particle in a quantum dot

Quantum dots are confined in all three dimensions and therefore has a potential with a minimum. The simplest way to describe the potential is to use the potential of a harmonic oscillator

$$V_{HO}(r) = \frac{m^*\omega^2 r^2}{2}, \tag{2.1}$$

where m^* is the effective mass of the electron. This model has shown to be a good approximation [3]. It is commonly used and is used in [4].

The electrons in quantum rings and dots belong to the conduction band of the semiconductor. The effective mass approximation takes their interaction with the lattice, the electrons in the valence band and the electrons in the core band into account. Instead of using the electron mass m_e, an effective mass m^* is used. For GaAs the effective mass is $m^* = 0.067m_e$.

The Schrödinger equation in Cartesian coordinates for one particle in a two dimensional harmonic oscillator can then be written

$$\left(-\frac{\hbar^2}{2m^*}\left(\frac{\partial^2}{\partial x^2}+\frac{\partial^2}{\partial y^2}\right)+\frac{m^*\omega^2(x^2+y^2)}{2}\right)\Psi(x,y) = E\Psi(x,y). \tag{2.2}$$

The analytical solution to equation (2.2) that corresponds to the lowest energy is

$$\Psi_{HO}(x,y) = Ne^{-\frac{m^*\omega}{2\hbar}(x^2+y^2)}, \tag{2.3}$$

where N is a normalization constant.

In cylindrical coordinates ($x = r\cos(\theta)$, $y = r\sin(\theta)$) with a potential that is circular symmetric the wave function can be divided into one radial and one angular part, $\Psi(x, y) = f_{m_l}(r)e^{im_l\theta}$. Equation (2.2) then becomes

$$\left(-\frac{\hbar^2}{2m^*}\left(\frac{\partial^2}{\partial r^2} + \frac{1}{r}\frac{\partial}{\partial r} + \frac{1}{r^2}\frac{\partial^2}{\partial\theta^2}\right) + \frac{m^*\omega r^2}{2}\right) f(r)e^{im_l\theta} = Ef(r)e^{im_l\theta}. \quad (2.4)$$

Changing variables to $\rho = \sqrt{\frac{m^*\omega}{\hbar}}r$ gives

$$\frac{\hbar\omega}{2}\left(-\frac{\partial^2}{\partial\rho^2} - \frac{1}{\rho}\frac{\partial}{\partial\rho} + \frac{m_l^2}{\rho^2} + \rho^2\right) f_{m_l}(\rho) = Ef_{m_l}(\rho), \quad (2.5)$$

with m_l being the angular quantum number.

2.1.2 One particle in a quantum ring

To describe a ring the potential for a shifted harmonic oscillator were used,

$$V_1(r) = \frac{m^*\omega^2(r - r_0)^2}{2}, \quad (2.6)$$

where r_0 is the radius of the ring. This model is commonly used [5]. Introducing the parameter

$$\rho_0 = \sqrt{\frac{m^*\omega}{\hbar}}r_0, \quad (2.7)$$

the Schrödinger equation for one particle in a ring can be written

$$\frac{\hbar\omega}{2}\left(-\frac{\partial^2}{\partial\rho^2} - \frac{1}{\rho}\frac{\partial}{\partial\rho} + \frac{m_l^2}{\rho^2} + (\rho - \rho_0)^2\right) f_{m_l}(\rho) = Ef_{m_l}(\rho). \quad (2.8)$$

This equation has no analytical solution.

2.1.3 One particle in two concentric rings

The third system to be studied was one particle in two concentric rings, that is one ring inside the other. The potential used for the two rings is

$$V_2(r) = \begin{cases} \frac{m^*\omega_1^2(r-r_{0,1})^2}{2} & r \leq r_c \\ \frac{m^*\omega_2^2(r-r_{0,2})^2}{2} & r > r_c \end{cases} \quad (2.9)$$

where $r_{0,1}$ and $r_{0,2}$ are the radii of the inner and outer ring and r_c is the point were the potentials are equal,

$$r_c = \frac{r_{0,2}\omega_2 + r_{0,1}\omega_1}{\omega_1 + \omega_2}. \quad (2.10)$$

This is the potential used in [6].

The reduced Schrödinger equation for this system is

$$\frac{\hbar\omega_1}{2}\left(-\frac{\partial^2}{\partial\rho^2}-\frac{1}{\rho}\frac{\partial}{\partial\rho}+\frac{m_l^2}{\rho^2}+\frac{\omega}{\omega_1}\rho^2\right)f_{m_l}(\rho)=Ef_{m_l}(\rho), \tag{2.11}$$

where

$$\omega=\begin{cases}\omega_1 & r\leq r_c\\ \omega_2 & r>r_c\end{cases} \tag{2.12}$$

2.1.4 Two particles

The Hamiltonian for two particles in a quantum dot, with the electron-electron interaction given by the Coulomb potential, is in Cartesian coordinates

$$H=\left(\sum_{i=1}^{2}-\frac{\hbar}{2m^*}\left(\frac{\partial^2}{\partial x_i^2}+\frac{\partial^2}{\partial y_i^2}\right)+\frac{m^*\omega^2\left(x_i^2+y_i^2\right)}{2}\right)+\frac{e^2}{4\pi\epsilon_0\epsilon_r}\frac{1}{\sqrt{(x_1-x_2)^2+(y_1-y_2)^2}}, \tag{2.13}$$

The dielectric constant, ϵ_0, is scaled with the relative dielectric constant, ϵ_r, of the semiconductor because of the effective mass approximation. The relative dielectric constant of GaAs is $\epsilon_r=12.4$.

Introducing the reduced variables $\overline{x}=\sqrt{\frac{m^*\omega}{\hbar}}x$ and $\overline{y}=\sqrt{\frac{m^*\omega}{\hbar}}y$ the Schrödinger equation becomes

$$\left(\left(\sum_{i=1}^{2}-\frac{1}{2}\left(\frac{\partial^2}{\partial\overline{x}_i^2}+\frac{\partial^2}{\partial\overline{y}_i^2}\right)+\frac{\overline{x}_i^2+\overline{y}_i^2}{2}\right)+\frac{\lambda}{\rho_{12}}\right)\Psi(\overline{x}_1,\overline{x}_2,\overline{y}_1,\overline{y}_2)=\frac{E}{\hbar\omega}\Psi(\overline{x}_1,\overline{x}_2,\overline{y}_1,\overline{y}_2), \tag{2.14}$$

where ρ_{12} is the distance between the particles,

$$\rho_{12}=\sqrt{(\overline{x}_1-\overline{x}_2)^2+(\overline{y}_1-\overline{y}_2)^2}, \tag{2.15}$$

and λ is the ratio between the typical length of the harmonic oscillator, $\sqrt{\hbar/m^*\omega}$, and the typical length of the Coulomb interaction,

$$\lambda=\frac{m^*e^2}{4\pi\epsilon_0\epsilon_r\hbar^2}\sqrt{\frac{\hbar}{m^*\omega}}. \tag{2.16}$$

The importance of the electron-electron interaction can be varied by altering ω and the material dependent parameters m^* and ϵ_r. Increasing the value of λ corresponds to increasing the relative importance of the Coulomb interaction. For a given material and a fixed ω the value of λ is determined.

For example, for GaAs, $1a_B^* \approx 9.79$nm, where a_B^* is the effective Bohr radius

$$a_B^* = \frac{4\pi\hbar^2\epsilon_0\epsilon_r}{m^* e^2} = \frac{\epsilon_r m_e}{m^*} a_B, \tag{2.17}$$

and $\hbar\omega = 10$meV gives $\overline{x} = a_B^*\sqrt{m\omega/\hbar} \approx 1.7181$. With these parameters the energy for two particles in a two dimensional harmonic oscillator is $3.0\hbar\omega = 0.3$meV and $\lambda = 1.0889$.

For one and two rings, equation (2.14) is used with the potential for a harmonic oscillator replaced with (2.6) and (2.9) respectively.

2.2 Variational Monte Carlo Method

In the Variational Monte Carlo method, see e.g. [7], a trial wave function $\Psi_T(\mathbf{r};\alpha)$ is optimized with respect to some parameters $\alpha = \alpha_1, ..., \alpha_m$ to obtain an approximation of the true wave function. The best approximation of the true wave function minimizes the energy. Define the local energy, $E_L(\mathbf{r};\alpha)$, as

$$E_L(\mathbf{r};\alpha) = \frac{H\Psi_T(\mathbf{r})}{\Psi_T(\mathbf{r})}. \tag{2.18}$$

When the trial wave function equals the exact wave function the local energy is constant and the variance of the energy is zero. The expectation value of the energy, $\langle E(\alpha)\rangle$, can be obtained from the local energy as

$$\langle E(\alpha)\rangle = \frac{\int \Psi_T^2(\mathbf{r}) E_L(\mathbf{r};\alpha)\mathrm{d}\mathbf{r}}{\int \Psi_T^2(\mathbf{r})\mathrm{d}\mathbf{r}}. \tag{2.19}$$

The minima of the energy and variance will not lie on the same point when the trial wave function is not equal to the exact wave function. To get a good approximation of the wave function both the energy and the variance needs to be minimized, in this thesis by minimizing $\langle E(\alpha)\rangle + \mathrm{var}(\langle E(\alpha)\rangle)$.

Computing the integral in equation (2.19) using uniformly distributed points would be very inefficient since many of the points would be in places were the integrand is small. A better choice is to use the Metropolis method [8]. The Metropolis algorithm consists of a random walk were each step is accepted or rejected with a certain probability. The idea is to sample points using a distribution so that an area in configuration space has a larger likelihood of being sampled the larger the values of the function are in that area.

The trial wave function is calculated for a large number of random points distributed according to

$$P(\mathbf{r}) = \frac{\Psi_T^2(\mathbf{r})}{\int \Psi_T^2(\mathbf{r}) \mathrm{d}\mathbf{r}}. \tag{2.20}$$

At every point the local energy is computed. The expectation value of the energy is then obtained from the average of the local energy. The variance of the energy is calculated from $\langle E^2 \rangle - \langle E \rangle^2$.

To sample from the distribution given by equation (2.20) random walks are made in the configuration space using a large number of walkers. To begin with the trial wave function is chosen and initial guesses for the parameters are made. The following is done for all the walkers.

- Place the walker at a random position and compute the initial wave function. Repeat the following three steps many times:
- Do a trial move and compute the new wave function.
- Compute the ratio $p = (\psi/\psi_{old})^2$. If $p \geq 1$ the trial move is accepted, otherwise it is accepted with a probability p.
- Compute the local energy

When all the walkers have been looped over, the average of the expectation value of the energy, and the average variance is computed as well as the standard deviations. The standard deviation of the energy is computed from

$$\sigma_{\langle E \rangle} = \sqrt{\left\langle \langle E \rangle^2 \right\rangle - \left\langle \langle E \rangle \right\rangle^2}. \tag{2.21}$$

The standard deviation of the variance is computed in a similar way. The standard deviations give the statistical error that can be reduced by a longer simulation (more walkers or more iterations). Since the variance is zero for the true wave function it is a measure of the systematic error. The uncertainty written for the results of the energy and the variance will be the statistical error.

To ensure that the result doesn't depend on the starting position, a number of the first data points for each walker are removed.

Then the parameter α is varied according to some minimization routine and the procedure is done all over again until the minimum of $\langle E(\alpha) \rangle + \mathrm{var}(\langle E(\alpha) \rangle)$ has been found with the wanted accuracy.

Each trial move displaces the walker with $\Delta(x - 0.5)$, where x is a random number between 0.0 and 1.0 and Δ is the step size. The steps size was chosen such that the acceptance ratio was approximately 0.5 to get an efficient sampling.

It is important to choose a good trial wave function since it determines the success of the simulation. Several different trial wave functions were therefore tried and compared for the different systems.

2.3 Minimization routines

For the minimization in one dimension Golden Section Search, as given in Numerical recipes in C, [9], was used. The routine is given three points x_a, x_b and x_c such that $f(x_a) > f(x_b)$ and $f(x_c) > f(x_b)$ and x_a and x_c are on opposite sides of the minimum. If the distance between the points x_c and x_b is greater than the distance between the points x_a and x_b, another point x_n is placed between x_c and x_b, else it is placed between x_a and x_b. The point x_b or x_n for which the function value is the lowest is made the new outer point and the other point of the two is made the new middle point. Thereafter a new point is placed between the unchanged outer point and the middle point. These steps are looped over until the distance between the two outer points are small enough given a tolerance.

When minimizing in several dimensions, Powell's (Direction set) method was used, as given in Numerical recipes in C, [9]. The method starts with initial guesses for the point of the minimum, $\mathbf{P}_0$, and a set of directions, $\mathbf{n}_0$, e.g. the unit vectors. In each direction the minima is bracketed by taking the initial point $\mathbf{P}_0$, a point further along the direction $\mathbf{P}_0 + \mathbf{n}$ and then trying to find a third point so that two of the points are on the opposite side of the minimum. A one dimensional minimization routine, in this case Golden Section Search, is used to find the scalar a that minimizes $f(\mathbf{P}+a\mathbf{n})$, where f is the function to be minimized, for all directions $\mathbf{n}$. In which direction the biggest decrease occurred and the magnitude of the decrease Δf is stored. After every minimization the old points are replaced by the new points $\mathbf{P}_N = \mathbf{P}_0 + a\mathbf{n}$ and the old direction is replaced by $\mathbf{n}_N = a\mathbf{n}$.

A new direction to minimize along is computed from average of the new and the old positions, $\mathbf{n}_A = \mathbf{P}_N - \mathbf{P}_0$. To check whether to use the new direction an extrapolated point, $\mathbf{P}_E$, is computed along the new direction, $\mathbf{P}_E = 2\mathbf{P}_N - \mathbf{P}_0$. If $f(\mathbf{P}_E) \geq f(\mathbf{P}_0)$ the new direction is rejected. The new direction is also rejected if $2(f(\mathbf{P}_0)-2f(\mathbf{P}_N)+f(\mathbf{P}_E))(f(\mathbf{P}_0)-f(\mathbf{P}_N)-\Delta f)^2 \geq (f(\mathbf{P}_N) - f(\mathbf{P}_0))^2\Delta f$. In this case, either there is a large second derivative and the current position is close to the minimum in the new direction, or the decrease in the new direction was not mainly caused by a decrease in any of the directions used to compute the new direction. If the direction is accepted, the direction that had the biggest decrease is replaced by the new direction. The direction with the biggest decrease will probably be a large

part of the new direction and replacing it will reduce the risk that the directions become linearly dependent. If the directions become linearly dependent the routine will only find the minimum in a subspace of the full space. These steps are done until the difference between $\mathbf{P}_0$ and $\mathbf{P}_n$ are small enough given a tolerance.

Chapter 3

One particle

3.1 One particle in a quantum dot

The Schrödinger equation for one particle in a two dimensional harmonic oscillator is analytically solvable and the system is used to test the routine. The trial wave function was chosen such that the analytical solution is in its variational subspace,

$$f_T^{HO}(\rho;\alpha) = e^{-\rho^2\alpha}. \tag{3.1}$$

The local energy with trial wave function (3.1) with $m_l = 0$ computed using equation (2.18), is

$$E_{L,HO}(\rho,\alpha) = 2\alpha + \frac{1}{2\rho^2} + 2\alpha^2 - \rho^2. \tag{3.2}$$

Because of the cylindrical coordinates boundary conditions were implemented such that if the walker after the trial move is at a position less than 0.0 , the walker is moved back inside the same distance as it was outside the box.

The walkers were initially placed on random positions between 0 and 3.5.

The Monte Carlo cycle were preformed 60000 times. Data were begun to be sampled after 5000 iterations and 4000 walkers were used. The results (with $m_l = 0$) for the parameter α, the energy and the variance are

$$\alpha_{HO,1} = 0.49996 \tag{3.3}$$

$$\langle E\rangle_{HO,1} = (0.99999999 \pm 0.00000005)\hbar\omega \tag{3.4}$$

$$\mathrm{var}(\langle E\rangle)_{HO,1} = (5.9987 \pm 0.002) \times 10^{-9}\hbar^2\omega^2 \tag{3.5}$$

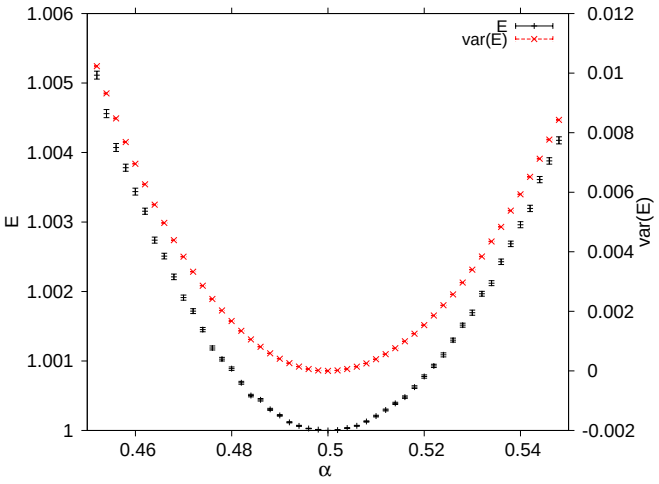

Figure 3.1: The energy and the variance as a function of the variational parameter α for one particle in a quantum dot with $m_l = 0$. The energy is in units of $\hbar\omega$.

The analytical value for the energy is

$$E_G^{HO,1} = 1.0\hbar\omega. \tag{3.6}$$

The result agrees very well with the analytical result.

Both the energy and the variance has a minimum for $\alpha = 0.5$, see figure 3.1.

3.2 One particle in one ring

Initially two different trial wave functions were tested, both with two variational parameters. The first trial wave function is similar to the one used for the quantum dot, equation (3.1), but with ρ replaced with $\rho - \rho_\alpha$,

$$f_T^{1,1}(\rho; \alpha, \rho_\alpha) = e^{-(\rho-\rho_\alpha)^2\alpha}, \tag{3.7}$$

with α and ρ_α being the variational parameters. The local energy using this wave function is

$$E_{L,1} = \alpha - 2\alpha^2(\rho - \rho_\alpha)^2 + \frac{\alpha(\rho - \rho_\alpha)}{\rho} + \frac{1}{2}(\rho - \rho_0)^2. \tag{3.8}$$

The second one contains a polynomial term and has the variational parameters α and a_1,

$$f_T^{1,2}(\rho; \alpha, a_1) = e^{-(\rho-\rho_0)^2\alpha}(1 + a_1\rho)^2. \tag{3.9}$$

The local energy with this trial wave function is

$$E_{L,2} = \alpha - 2(\rho-\rho_0)^2\alpha^2 + \frac{4(\rho-\rho_0)\alpha a_1}{1+\rho a_1} - \frac{a_1^2}{(1+\rho a_1)^2} + \frac{1}{\rho}((\rho-\rho_0)\alpha - \frac{a_1}{1+\rho a_1}) + \frac{1}{2}(\rho-\rho_0)^2. \tag{3.10}$$

Since there are $1/\rho$ terms in the local energies, the boundary condition had to be modified so that the walkers can't visit the point $\rho = 0$. This was done by introducing a small number ϵ, so that the simulation box ends at ϵ instead of 0. The value of ϵ chosen was 10^{-20}. By varying ϵ and looking at the variance when using a radius of 0.5 it could be seen that this value did not affect the result.

To obtain good result for small radii three other trial wave functions with polynomial parts were tried. One of them is a combination of the two previous trial wave functions, with three variational parameters α, ρ_α and a_1,

$$f_T^{1,3}(\rho;\alpha,\rho_\alpha,a_1) = e^{-(\rho-\rho_\alpha)^2\alpha}\left(1+a_1\rho\right)^2. \tag{3.11}$$

A trial wave function with a ρ^2 term in the polynomial were also tried,

$$f_T^{1,4}(\rho;\alpha,\rho_\alpha,a_2) = e^{-(\rho-\rho_\alpha)^2\alpha}\left(1+a_2\rho^2\right)^2, \tag{3.12}$$

with α, ρ_α and a_2 being the variational parameters.

The final wave function to be tested is a combination of the previous ones, with four variational parameters

$$f_T^{1,5}(\rho;\alpha,\rho_\alpha,a_1,a_2) = e^{-(\rho-\rho_\alpha)^2\alpha}\left(1+a_1\rho+a_2\rho^2\right)^2. \tag{3.13}$$

The walkers were initially placed on random positions between $\rho_0 - 2.5$ and $\rho_0 + 2.5$. For small radii the walkers were initially placed between 0 and 2.5.

The simulations were done using 800 walkers. For each walker 60 000 iterations were done, of which the first 4000 data points were removed.

Table 3.1 and 3.2 shows the obtained energy and variance for a particle in a ring with radius 50 and 10 respectively, with $m_l = 0$, using the trial wave functions with two parameters, equations (3.7) and (3.9). The trial wave function with a polynomial term, equation (3.9), gave the lowest variance and the lowest energy and therefore the best result for both radii. The energies obtained using trial wave function (3.9) agrees well with the results obtained by diagonalization. For a large ring the expected result for the energy is $0.5\hbar\omega$, the energy of a one dimensional harmonic oscillator. The results obtained for radii 10 and 50 are close to this value.

The result for the energy and the variance for $\rho_0 = 3.0$ and $m_l = 0$ is shown in table 3.3 using the trial wave functions with two parameters,

f_T	$\langle E/\hbar\omega\rangle$	var$(\langle E/\hbar\omega\rangle)$
$f_T^{1,1}(\rho;\alpha,\rho_\alpha)$	$0.49995009 \pm 0.00000007$	$(4.771 \pm 0.003) \times 10^{-8}$
$f_T^{1,2}(\rho;\alpha,a_1)$	$0.49994997 \pm 0.00000001$	$(1.674 \pm 0.002) \times 10^{-9}$
Diagonalization	0.499949970	

Table 3.1: The energy and variance for a particle in a ring with radius 50.0 and $m_l = 0$ compared with the value obtained by diagonalization.

f_T	$\langle E/\hbar\omega\rangle$	var$(\langle E/\hbar\omega\rangle)$
$f_T^{1,1}(\rho;\alpha,\rho_\alpha)$	0.4987309 ± 0.0000001	$(2.234 \pm 0.008) \times 10^{-7}$
$f_T^{1,2}(\rho;\alpha,a_1)$	0.4987306 ± 0.0000001	$(2.058 \pm 0.006) \times 10^{-7}$
Diagonalization	0.49873073	

Table 3.2: The energy and variance for a particle in a ring with radius 10.0 and $m_l = 0$ compared with the value obtained by diagonalization.

equations (3.7) and (3.9), and the trial wave function with five parameters, equation (3.13). The variance is about the same for all three trial wave functions. The best value, obtained by equation (3.13), is slightly higher than the result obtained by diagonalization. The variance is much higher than for a ring with radius 10, which shows that there is a larger systematic error from the trial wave function used. Figure 3.2 shows the probability distribution for a ring with radius 3.0 using the three different trial wave functions. The difference between the trial wave functions is very small.

Table 3.4 shows the energy and variance for a particle in a ring with radius 2.0 and $m_l = 0$ using all five trial wave functions. The best result was obtained with trial wave function (3.13), as expected since it contains the most parameters. The trial wave functions with a ρ^2 term in the polynomial gave a much smaller variance than the other ones. The difference between trial wave functions (3.13) and (3.12) is quite small. Including a ρ term has

f_T	$\langle E/\hbar\omega\rangle$	var$(\langle E/\hbar\omega\rangle)$
$f_T^{1,1}(\rho;\alpha,\rho_\alpha)$	0.48297 ± 0.00001	$(2.3 \pm 0.2) \times 10^{-3}$
$f_T^{1,2}(\rho;\alpha,a_1)$	0.48294 ± 0.00001	$(2.7 \pm 0.6) \times 10^{-3}$
$f_T^{1,5}(\rho;\alpha,\rho_\alpha,a_1,a_2)$	0.48291 ± 0.00001	$(1.9 \pm 0.1) \times 10^{-3}$
Diagonalization	0.4824356	

Table 3.3: The energy and variance for a particle in a ring with radius 3.0 and $m_l = 0$ compared with the value obtained by diagonalization.

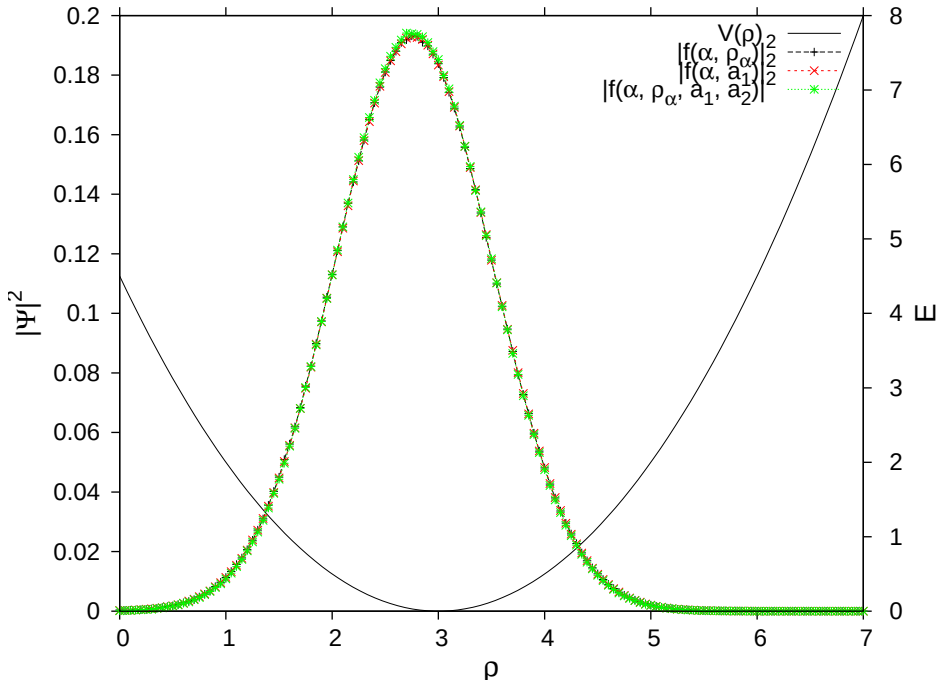

Figure 3.2: The probability distribution for a particle in a ring with radius 3.0 using trial wave functions (3.7), (3.9) and (3.13) with $m_l = 0$. The energy is in units of $\hbar\omega$.

f_T	$\langle E/\hbar\omega\rangle$	var$(\langle E/\hbar\omega\rangle)$
$f_T^{1,1}(\rho;\alpha,\rho_\alpha)$	0.46218 ± 0.00006	0.12 ± 0.03
$f_T^{1,2}(\rho;\alpha,a_1)$	0.45689 ± 0.00005	0.11 ± 0.03
$f_T^{1,3}(\rho;\alpha,\rho_\alpha,a_1)$	0.45892 ± 0.00006	$(8.4 \pm 0.9) \times 10^{-2}$
$f_T^{1,4}(\rho;\alpha,\rho_\alpha,a_2)$	0.448496 ± 0.000009	$(2.13 \pm 0.04) \times 10^{-3}$
$f_T^{1,5}(\rho;\alpha,\rho_\alpha,a_1,a_2)$	0.448285 ± 0.000007	$(1.11 \pm 0.08) \times 10^{-3}$
Diagonalization	0.4481174	

Table 3.4: The energy and variance for a particle in a ring with radius 2.0 and $m_l = 0$ compared with the value obtained by diagonalization.

f_T	$\langle E/\hbar\omega\rangle$	var$(\langle E/\hbar\omega\rangle)$
$f_T^{1,1}(\rho;\alpha,\rho_\alpha)$	0.65377 ± 0.00002	$(5.4 \pm 0.4) \times 10^{-3}$
$f_T^{1,2}(\rho;\alpha,a_1)$	0.65342 ± 0.00001	$(3.3 \pm 0.1) \times 10^{-3}$
$f_T^{1,4}(\rho;\alpha,\rho_\alpha,a_2)$	0.652901 ± 0.000007	$(8.2 \pm 0.3) \times 10^{-4}$
$f_T^{1,5}(\rho;\alpha,\rho_\alpha,a_1,a_2)$	0.652902 ± 0.000007	$(8.3 \pm 0.1) \times 10^{-4}$
Diagonalization	0.652794	

Table 3.5: The energy and variance for a particle in a ring with radius 0.5 with $m_l = 0$ compared with the value obtained by diagonalization.

thus a relatively small effect on the result. As for a ring with radius 3, the value obtained with diagonalization is slightly lower than the result obtained with $f_T^{1,5}(\rho;\alpha,\rho_\alpha,a_2,a_2)$ and the variance is quite high.

Figure 3.3 shows the probability distributions together with the potential. As can be seen, the potential is not a true ring. A ρ^2 term is needed for the asymmetric form of the wave function.

Figure 3.4 shows the probability distribution using trial wave functions (3.7), (3.9), (3.12) and (3.13) together with the potential with $\rho_0 = 0.5$ and $m_l = 0$. The potential is close to zero at $\rho = 0$ and is similar to the potential of an harmonic oscillator, but wider. The energy is therefore lower than for one particle in a two dimensional harmonic oscillator. Table 3.5 shows the result for the energy and the variance and the result for the energy using diagonalization. As for a ring with radius 2.0, the trial wave functions with a ρ^2 term gave a lower variance then the others. Trial wave functions (3.12) and (3.13) gave almost the same energy and variance. The energy obtained is a bit higher than the energy obtained with diagonalization. The difference is smaller than with $\rho_0 = 3$ and the variance is also lower.

Figure 3.5 shows the variance for different radii using the five different trial wave functions. Trial wave function (3.9) is better than (3.7) for large

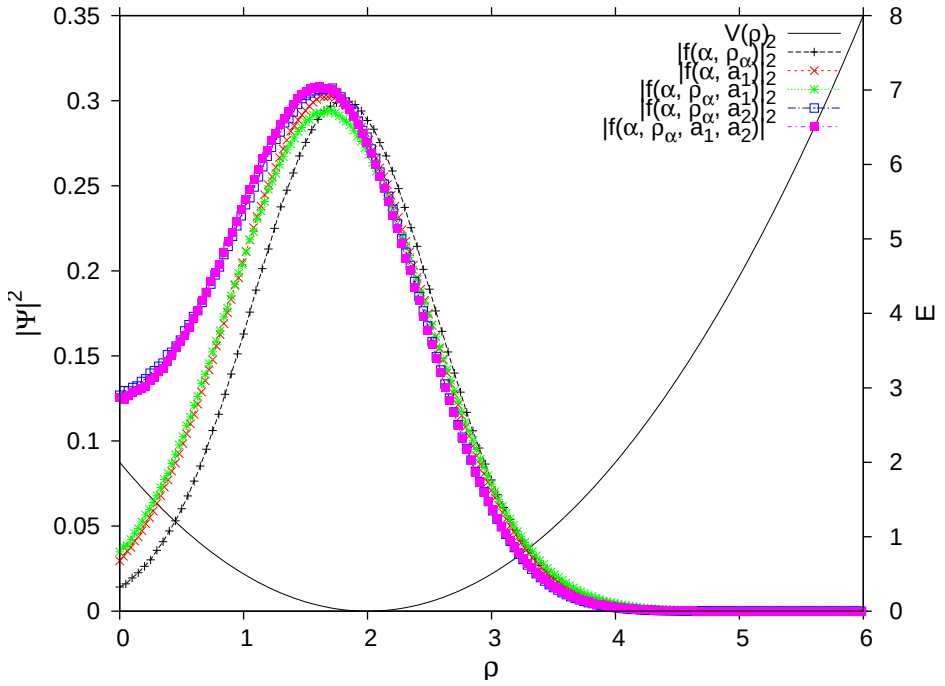

Figure 3.3: The probability distribution for a particle in a ring with radius 2.0 and $m_l = 0$ using trial wave functions (3.7), (3.9), (3.11), (3.12), and (3.13). The energy is in units of $\hbar\omega$.

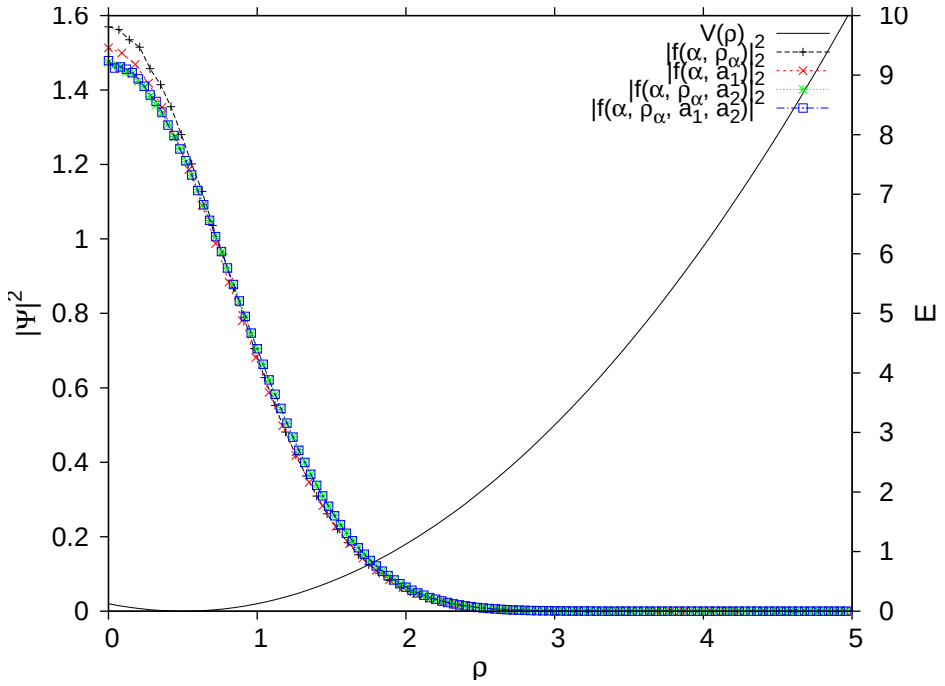

Figure 3.4: The probability distribution for a particle in a ring with radius 0.5 using trial wave functions (3.7), (3.9), (3.12), and equation (3.13) with $m_l = 0$. The energy is in units of $\hbar\omega$.

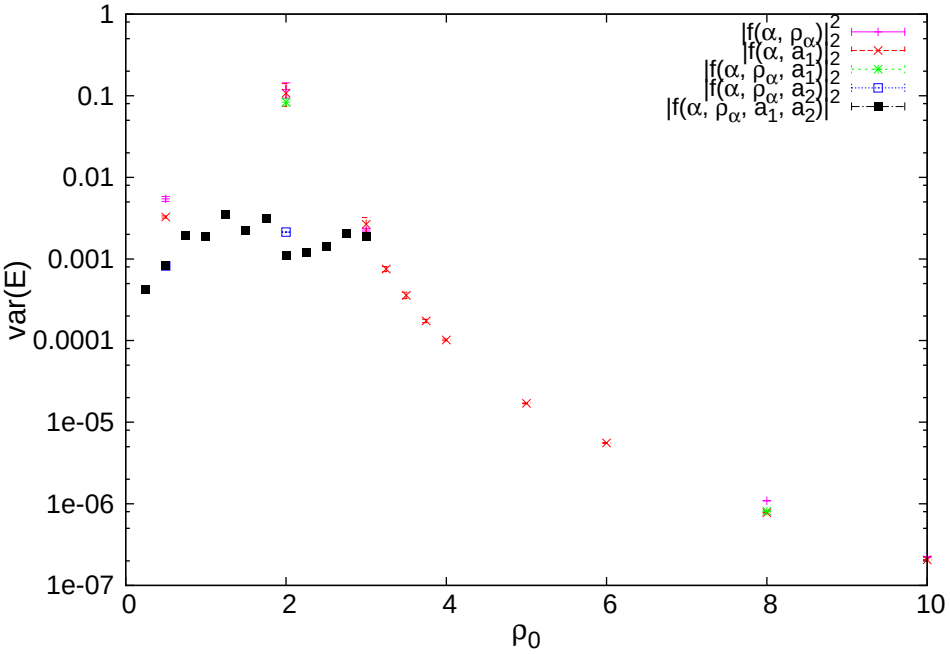

Figure 3.5: The variance as a function of ρ_0 for a one particle system using the different trial wave functions. The energy is in units of $\hbar\omega$.

radii and when $\rho_0 = 0.5$. When $\rho_0 = 2$ and $\rho_0 = 2$, the variance is about the same for both the trial wave functions. The combination of (3.9) and (3.7), trial wave function (3.11) was tried for two different radii, $\rho_0 = 2$ and $\rho_0 = 8$. Trial wave function (3.11) gives a lower variance than the two trial wave functions with two parameters when $\rho_0 = 2$. When $\rho_0 = 8$ (3.11) gives about the same variance as (3.9). The trial wave functions with a ρ^2 term gives the best result for $\rho_0 < 3$. For larger radii, when the potential is a true ring, a ρ^2 term is no longer needed. For efficiency reasons, one wants to use as few variational parameters as possible. Trial wave function (3.9) was therefore used to calculate the energies for $\rho_0 > 3$, since adding more parameters gave almost no change in the variance for larger radii. After $\rho_0 = 3$, the variance quickly gets smaller as the radius increases. The true wave function becomes more similar to the wave function of a one dimensional harmonic oscillator, which lies in the variational subspace of the trial wave functions used. The variance also deceases for small radii, since the true wave function becomes similar to the wave function of a two dimensional harmonic oscillator.

Figure 3.6 shows the energy as a function of the radius of the ring using trial wave function (3.13) for $\rho_0 < 3.0$ and trial wave function (3.9) for $\rho_0 \geq 3.0$. The energy initially drops quickly. Around $\rho_0 = 1.5$ the energy has

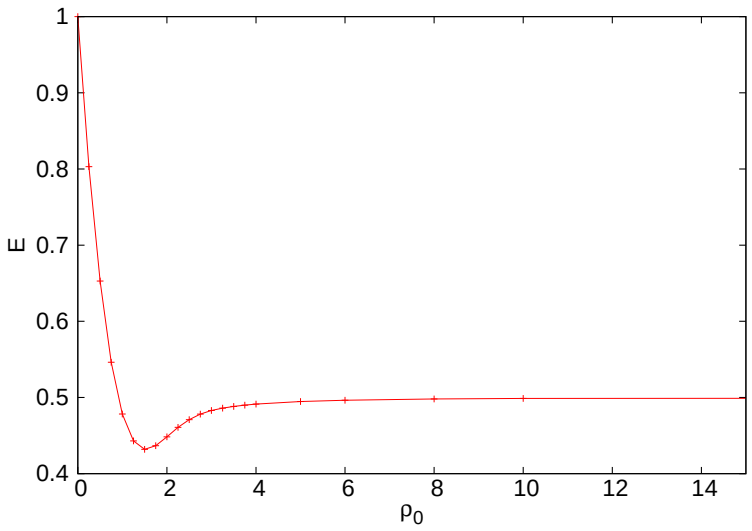

Figure 3.6: The energy as a function of the radius of the ring for a one particle system. The energy is in units of $\hbar\omega$.

a minimum and from there it slowly increases and approaches $0.5\hbar\omega$. When the radius increases from 0 the volume of the ring gets lager and the energy therefore decreases. When a true ring begins to form, the energy starts to increase. For a large enough radius the ring bends so slowly that for a particle in the ring, the potential will appear like a straight line. Without any angular dependency, this will make the system similar to a one dimensional harmonic oscillator.

Figure 3.7 shows the obtained parameters for $f_T^{1,2}(\rho, \alpha, a_1)$ as functions of the radius. When the radii gets large the wave function should become similar to the wave function for a one dimensional harmonic oscillator with $\alpha = 0.5$ and $a_1 = 0.0$. From the figure one can see that the parameters approache these values as the radii increases.

Table 3.6 shows the energy and variance using all five trial wave functions for a ring with radius 3.0 and $m_l = 1$ compared with the energy obtained with diagonalization. The trial wave functions with two parameters, (3.7) and (3.9), gave large variances. A much smaller variance was obtained with trial wave function (3.13). The resulting energy is a bit higher than the energy obtained with diagonalization. The difference between the result and the value obtained by diagonalization is greater for $m_l = 1$ than $m_l = 0$, see table 3.3. The variance is also larger for $m_l = 1$. The trial wave functions thus describe systems with $m_l = 1$ less well. Figure 3.8 shows the probability distributions compared with the probability distribution for $m_l = 0$

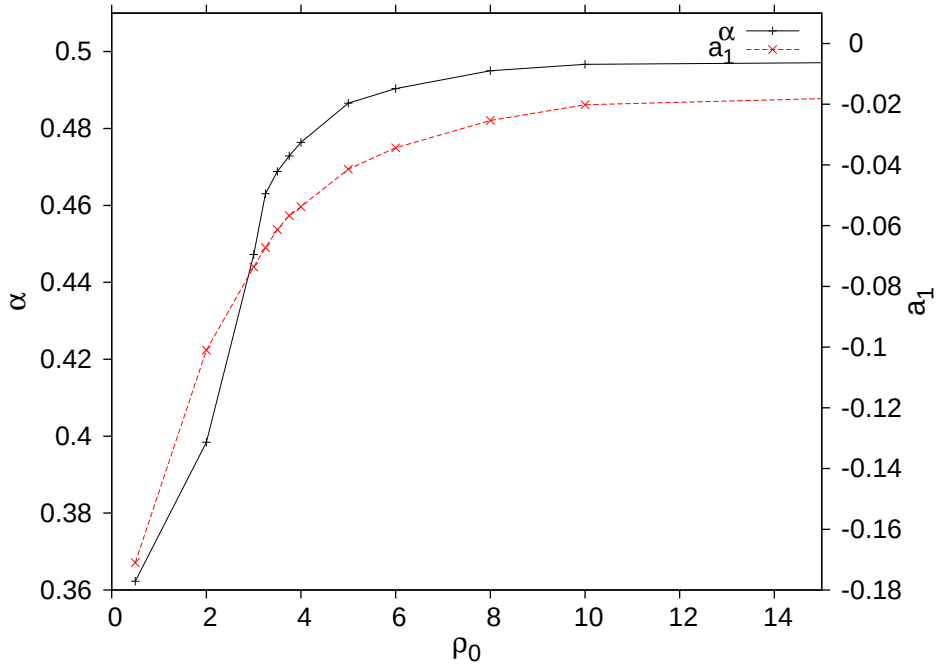

Figure 3.7: The parameters using trial wave function $f_T^{1,2}(\rho, \alpha, a_1)$ as functions of the radius with $m_l = 0$.

using trial wave function (3.13). The probability distribution for $m_l = 1$ is slightly shifted away from the origin. The probability distributions for the five different trial wave functions are quite similar.

3.3 One particle in two concentric rings

Two trial wave functions were tested, one with three variational parameters and one with five parameters,

$$f_T^{2,1}(\rho; \rho_{\alpha_1}, \rho_{\alpha_2}, c) = e^{-(\rho-\rho_{\alpha_1})^2/2} + ce^{-(\rho-\rho_{\alpha_2})^2/2}, \tag{3.14}$$

and

$$f_T^{2,2}(\rho; \alpha_1, \rho_{\alpha_1}, \alpha_2, \rho_{\alpha_2}, c) = e^{-(\rho-\rho_{\alpha_1})^2\alpha_1} + ce^{-(\rho-\rho_{\alpha_2})^2\alpha_2}. \tag{3.15}$$

The walkers were initially placed on random positions between $\rho_{0,1} - 2.5$ and $\rho_{0,2} + 2.5$. The number of walkers used were 400. For each walker 60 000 iterations were done, of which the first 4000 were removed.

The result for the energy and variance using trial wave functions 3.14 and 3.15 are shown in table 3.7 with $\rho_{0,1} = 3$, $\rho_{0,2} = 6$, $\omega_1 = \omega_2 = 1.0$ and $m_l = 0$.

f_T	$\langle E/\hbar\omega \rangle$	var($\langle E/\hbar\omega \rangle$)
$f_T^{1,1}(\rho;\alpha,\rho_\alpha)$	0.55212 ± 0.00003	$(2 \pm 2) \times 10^{-2}$
$f_T^{1,2}(\rho;\alpha,a_1)$	0.55771 ± 0.00003	$(1.2 \pm 0.2) \times 10^{-2}$
$f_T^{1,3}(\rho;\alpha,\rho_\alpha,a_1)$	0.55245 ± 0.00002	$(7 \pm 2) \times 10^{-3}$
$f_T^{1,4}(\rho;\alpha,\rho_\alpha,a_2)$	0.55293 ± 0.00002	$(7 \pm 3) \times 10^{-3}$
$f_T^{1,5}(\rho;\alpha,\rho_\alpha,a_1,a_2)$	0.55205 ± 0.00002	$(3.76 \pm 0.04) \times 10^{-3}$
Diagonalization	0.55095	

Table 3.6: The energy and variance for a particle in a ring with radius 3.0 and $m_l = 1.0$

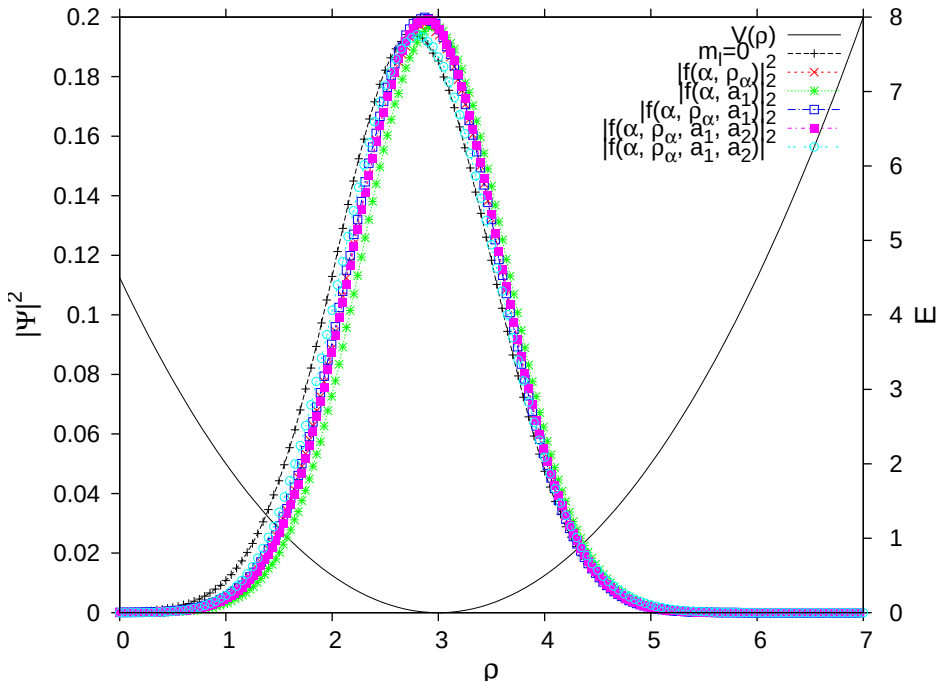

Figure 3.8: The probability distribution for a particle in a ring with radius 3.0 and $m_l = 1$ compared with the result for $m_l = 0$ using trial wave function (3.13). The energy is in units of $\hbar\omega$.

f_T	$\langle E/\hbar\omega_1 \rangle$	var($\langle E/\hbar\omega_1 \rangle$)
$f_T^{2,1}(\rho;\rho_{\alpha_1},\rho_{\alpha_2})$	0.39242 ± 0.00003	$(5.0 \pm 0.4) \times 10^{-3}$
$f_T^{2,2}(\rho;\alpha_1,\rho_{\alpha_1},\alpha_2,\rho_{\alpha_2})$	0.39156 ± 0.00001	$(3.39 \pm 0.08) \times 10^{-3}$
Diagonalization	0.39098	

Table 3.7: The energy and variance for one particle in two rings, with $\rho_{0,1} = 3$, $\rho_{0,2} = 6$ and $\omega_1 = \omega_2 = 1.0$, using trial wave functions (3.14) and (3.15) compared with the value obtained by diagonalization.

$\rho_{0,2}$	$\langle E/\hbar\omega_1 \rangle$	var($\langle E/\hbar\omega_1 \rangle$)	$P_{\rho<\rho_{1,0}}$
6.0	0.39156 ± 0.00001	$(3.39 \pm 0.08) \times 10^{-3}$	0.52229 ± 0.00002
7.0	0.46513 ± 0.00001	$(1.48 \pm 0.307) \times 10^{-3}$	0.70293 ± 0.00001
8.0	0.48277 ± 0.00002	$(2.3 \pm 0.2) \times 10^{-3}$	0.99976 ± 0.00002

Table 3.8: The energy and variance for one particle in two rings, with $\rho_{0,1} = 3$ and $\omega_1 = \omega_2 = 1.0$.

The variance is slightly lower when using five parameters than when using three. There is a visible difference in the probability distribution, see figure 3.9. The energy obtained with trial wave function (3.15 is slightly higher than the result obtained by diagonalization. The variance is higher than the variance for one ring with $m_l = 0$. Trial wave function (3.15) is the one used in the rest of this section.

The probability for the particle to be in the inner ring, $P_{\rho<\rho_c}$, were calculated from,

$$P_{\rho<\rho_c} = \int_0^{\rho_c} |\Psi(\rho)|^2 \mathrm{d}\rho, \tag{3.16}$$

where ρ_c is given by equation (2.10).

Table 3.8 shows the energy, variance and the probability to be in the inner ring for three different values of the radius of the outer ring with $\rho_{0,1} = 3$, $\omega_1 = \omega_2 = 1.0$ and $m_l = 0$. The probability of the particle to be in the inner ring increases when the radius of the outer ring gets larger. With $\rho_{0,2} = 6.0$, the probability for the particle to be in the inner ring is about 0.5. This probability increases to almost 1.0 when $\rho_{0,2} = 8.0$. Figure 3.11 shows the probability distributions with the three different values of $\rho_{0,2}$. The potentials the three different outer radii is shown in figure 3.10.

When the radius of the outer ring increases the energy gets larger. For $\rho_{0,2} = 8.0$ the energy is equal to the energy of one particle in a ring with radius 3. When $\rho_{0,2} = 6.0$ the energy is lower than the minimum energy for a particle in one ring, since the volume of the potential is larger.

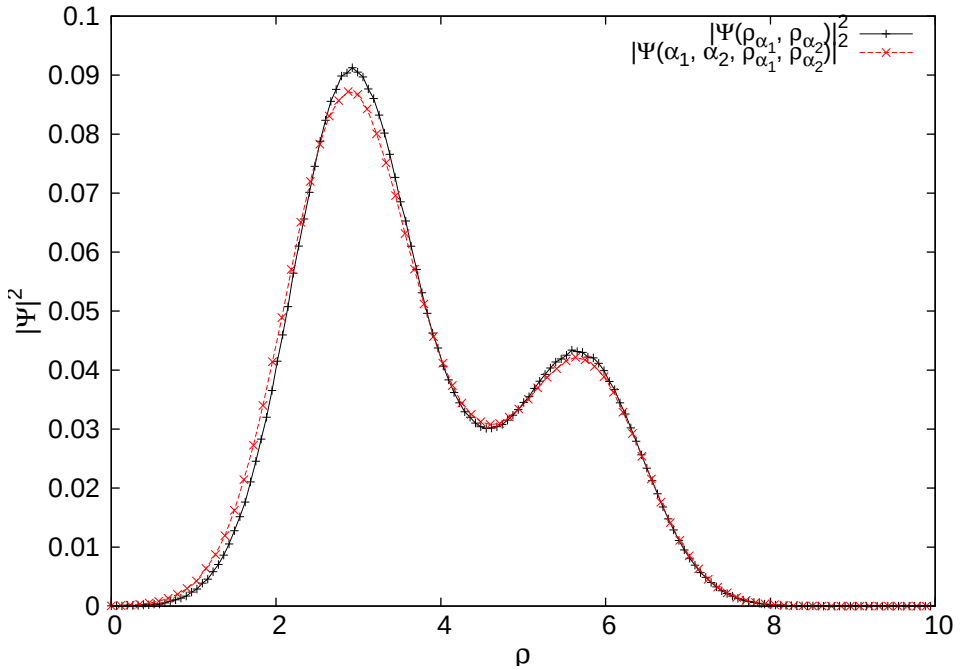

Figure 3.9: The probability distribution using trial wave functions (3.14) and (3.15) for $\rho_{0,1} = 3.0$, $\omega_1 = \omega_2 = 1$.

ω_2/ω_1	$\langle E/\hbar\omega_1 \rangle$	var$(\langle E/\hbar\omega_1 \rangle)$	$P_{\rho<\rho_c}$
0.5	0.21069 ± 0.00001	$(1.14 \pm 0.01) \times 10^{-3}$	0.15874 ± 0.00001
1.0	0.39156 ± 0.00001	$(3.39 \pm 0.08) \times 10^{-3}$	0.52229 ± 0.00002
2.0	0.47358 ± 0.00003	$(2.4 \pm 0.1) \times 10^{-3}$	0.98033 ± 0.00002

Table 3.9: The energy and variance for one particle in two rings, $\rho_{0,1} = 3.0$, $\rho_{0,2} = 6.0$.

Figure 3.13 shows the probability distribution for three different values of ω_2, in units of ω_1, with $\rho_{0,1} = 3.0$, $\rho_{0,2} = 6.0$ and $m_l = 0$. The likelihood for the particle to be in the inner ring decreases and the energy increases when the value of ω_2 increases, as expected since a larger ω corresponds to a smaller volume of the potential, see figure 3.12.

Table 3.10 shows the energy with $\rho_{0,1} = 10.5256$, $\rho_{0,2} = 15.7884$, $\omega_1 = 35$meV, $m^* = 0.067$ and $\epsilon_r = 12.4$ compared with the energies obtained by exact diagonalization. The result obtained by variational Monte Carlo is in good agreement with the result obtained by diagonalization. The variance is also very small, see table 3.11.

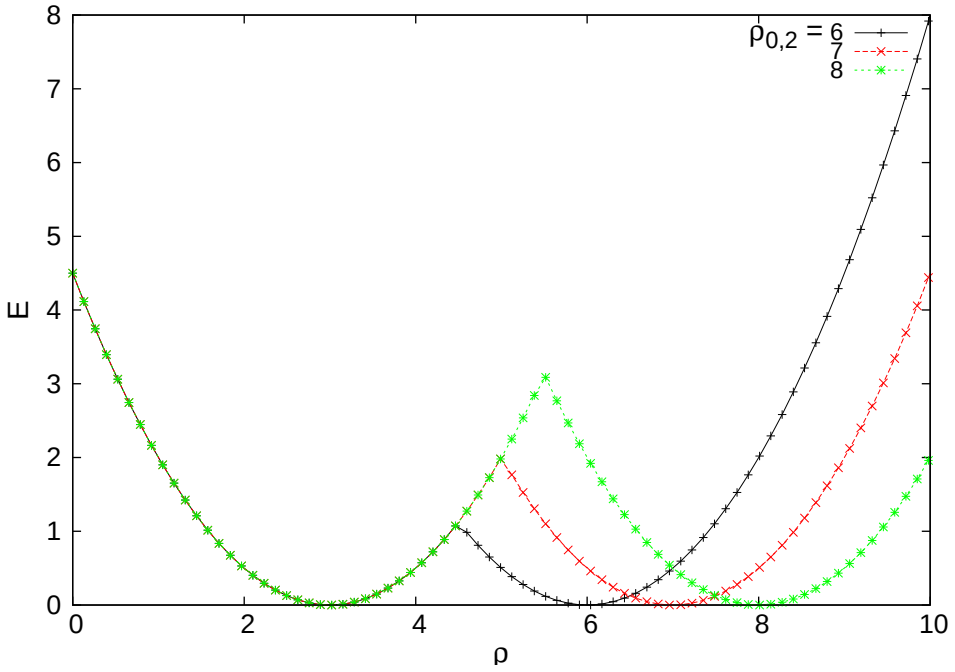

Figure 3.10: The potentials for two rings with three different values for $\rho_{0,2}$, $\rho_{0,1} = 3.0$ and $\omega_1 = \omega_2 = 1.0$. The energy is in units of $\hbar\omega_1$.

$\hbar\omega_2$(meV)	$E/\hbar\omega_1$	$\langle E/\hbar\omega_1\rangle$
40.0	0.498788	0.498793 ± 0.000001
35.15	0.498097	0.498126 ± 0.000003

Table 3.10: The energy for one particle in two rings, with $r_{0,1} = 60$nm, $r_{0,2} = 90$nm, $\hbar\omega_1 = 35$meV, $m^* = 0.067$ and $\epsilon_r = 12.4$ compared with the energies obtained by diagonalization in the first column.

$\hbar\omega_2$ (meV)	var($\langle E/\hbar\omega_1\rangle$)	$P_{\rho<\rho_c}$
40.0	$(2.1 \pm 0.1) \times 10^{-5}$	0.999751 ± 0.000001
35.15	$(9.98 \pm 0.08) \times 10^{-5}$	0.849079 ± 0.000003

Table 3.11: The energy and variance for one particle in two rings, $r_{0,1} = 60$nm, $r_{0,2} = 90$nm, $\hbar\omega_1 = 35$meV and the effective mass and dielectric constant of GaAs.

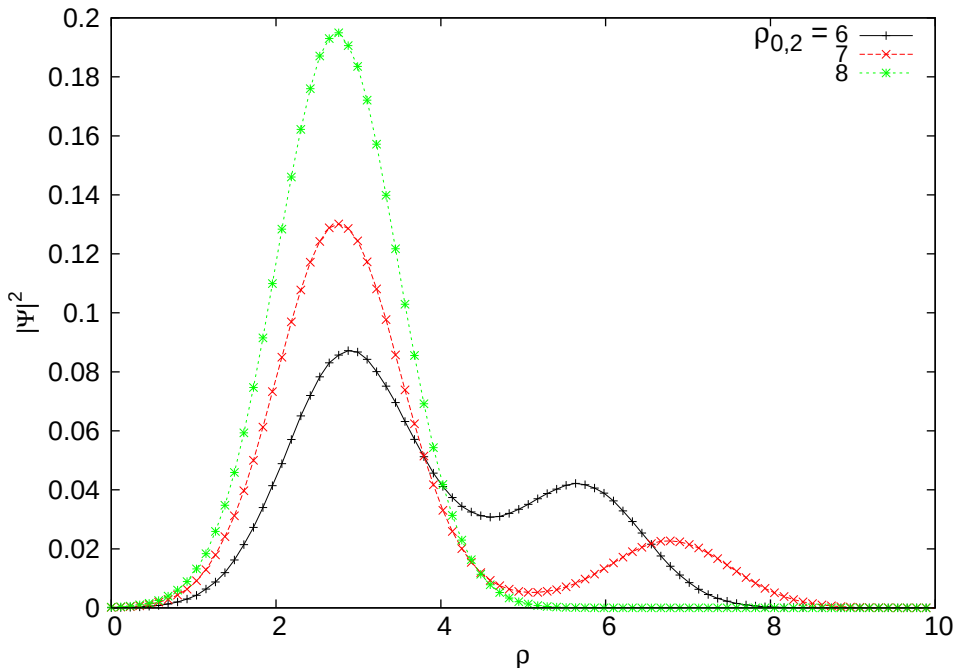

Figure 3.11: The probability distribution using equation (3.15) for three different values of $\rho_{0,2}$ with $\rho_{0,1} = 3.0$ and $\omega_1 = \omega_2 = 1.0$.

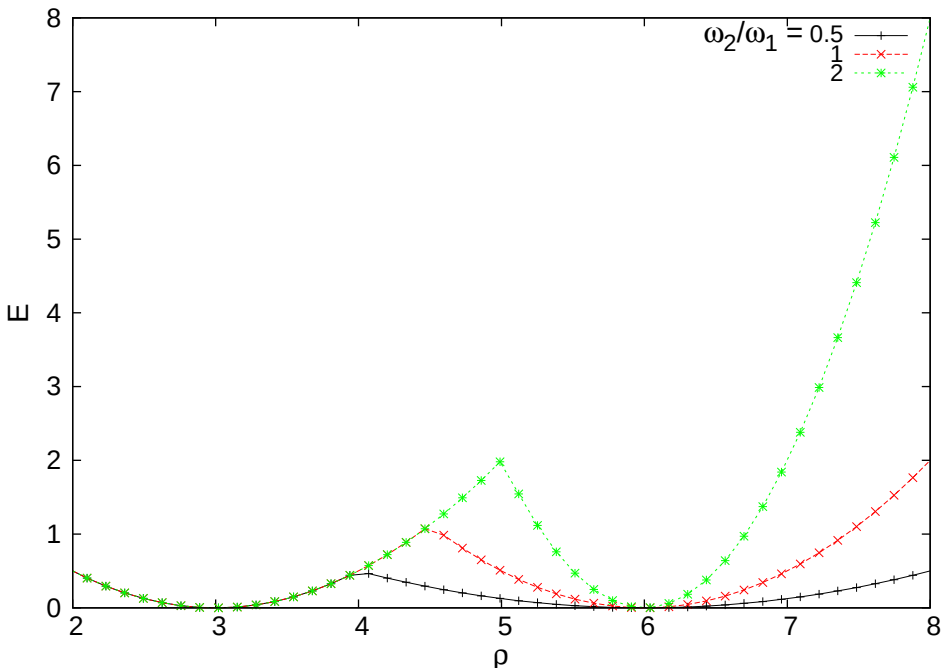

Figure 3.12: The potential for three different values of ω_2/ω_1 with $\rho_{0,1} = 3.0$ and $\rho_{0,2} = 6.0$. The energy is in units of $\hbar\omega_1$.

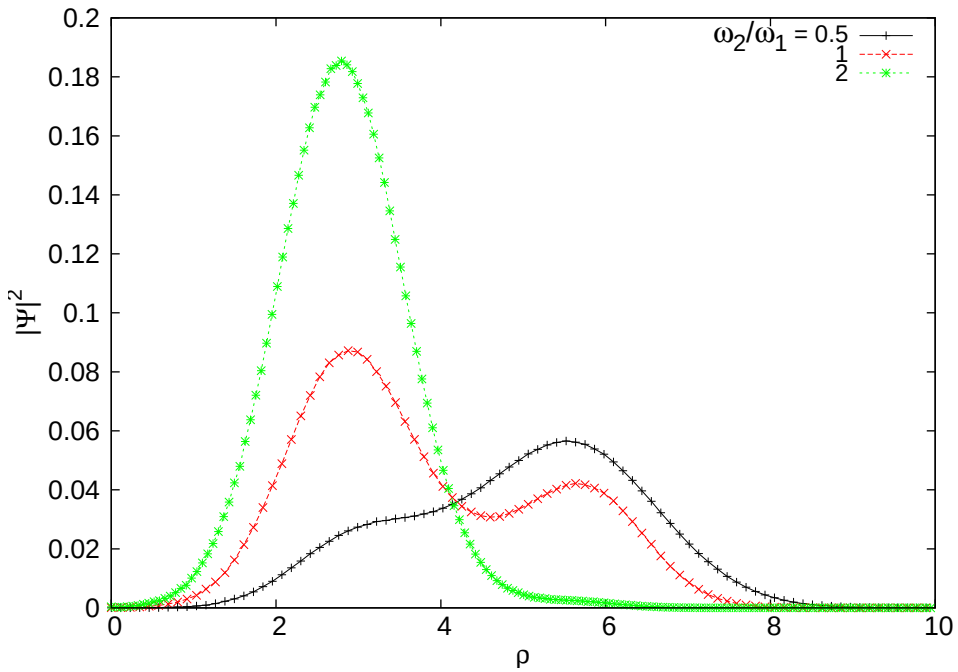

Figure 3.13: The probability distribution using equation (3.15) for three different values of ω_2, in units of ω_1, with $\rho_{0,1} = 3.0$ and $\rho_{0,2} = 6.0$.

Chapter 4

Two particles

4.1 Two particles in a quantum dot

For two particles, the trial wave function consist of the trial wave functions for the individual particles and a term describing the correlation. A commonly used way of describing the electron-electron interaction is to use a so called Jastrow function [10] (see e.g. [11])

$$\exp\left(\frac{\lambda\rho_{12}}{1+\beta\rho_{12}}\right), \tag{4.1}$$

where ρ_{12} is the distance between the particles and β is a variational parameter.

The trial wave function used for two particles in a quantum dot with equation (3.1) for the single particle wave functions and equation (4.1) for the correlation part is

$$\Psi_T^{HO,2}(\overline{x}_1, \overline{x}_2, \overline{y}_1, \overline{y}_2; \alpha, \beta) = e^{-(\rho_1^2+\rho_2^2)\alpha} e^{\frac{\lambda\rho_{12}}{1+\beta\rho_{12}}}. \tag{4.2}$$

It is assumed that the particles have opposite spins. The particles can therefore be in the same state and the same variational parameter for the single particle part can be used for both particles.

The single particle part is written in cylindrical coordinates and the correlation part in Cartesian coordinates to simplify the calculation of the local energy, see the appendix. The trial moves were done in the xy-plane and the x and y position of one particle were changed at every trial move.

The result was obtained with 900000 iterations, of which the first 16000 data points removed, and 1600 walkers. The step size was set to 3.5 and the box size to 7.0. The walkers were initially placed between -2.5 and 2.5 in the

x and y directions. The parameters obtained were

$$\alpha_{HO,2} = 0.4918, \beta_{HO} = 0.4128 \tag{4.3}$$

The result for the expectation value of the energy was

$$\langle E \rangle_{HO,2} = (3.00041 \pm 0.00003)\hbar\omega \tag{4.4}$$

and the result for the variance was

$$\mathrm{var}(\langle E \rangle)_{HO,2} = (1.595 \pm 0.001) \times 10^{-3}\hbar^2\omega^2. \tag{4.5}$$

The exact value for the ground state energy for $\lambda = 1$ was calculated by Taut [12], with the result

$$E_G^{HO,2} = 3.0\hbar\omega. \tag{4.6}$$

The expectation value of the distance between the particles, $\langle \rho_{12} \rangle$, was calculated from the local value, equation (2.15) on the same way as the expectation value of the energy, equation (2.19),

$$\langle \rho_{12} \rangle = \frac{\int \Psi_T^2(\rho_1, \rho_2)\rho_{12}(\rho_1, \rho_2)\mathrm{d}\rho_1\mathrm{d}\rho_2}{\int \Psi_T^2(\rho_1, \rho_2)\mathrm{d}\rho_1\mathrm{d}\rho_2}. \tag{4.7}$$

The result is

$$\langle \rho_{12} \rangle_{HO} = 1.6275 \pm 0.0004. \tag{4.8}$$

The relative probability distribution, $P(\overline{x}_1, \overline{y}_1)$, for one of the particles with the position of the other particle held fixed at the angle $\theta = \pi/4$ were calculated from the obtained wave functions by

$$P(\overline{x}_1, \overline{y}_1) = \int_0^\infty |\Psi(\overline{x}_1, \overline{y}_1, \overline{x}_2, \overline{y}_2 = \overline{x}_2)|^2 \mathrm{d}\overline{x}_2. \tag{4.9}$$

Figure 4.1 shows the relative probability distribution using three different values λ calculated using equation (4.9). For $\lambda = 0$ the probability distribution is a circle centred at the origin. The stronger the relative electron-electron interaction is the more shifted away from the origin the probability distribution becomes.

4.2 Two particles in one ring

For two particles in one ring the potential term in the Hamiltonian for a quantum dot, equation (2.13), was replaced by the potential for a ring, equation (2.6). A trial wave function using equation (3.7) for the single particle wave function was used when $\rho_0 \geq 3$,

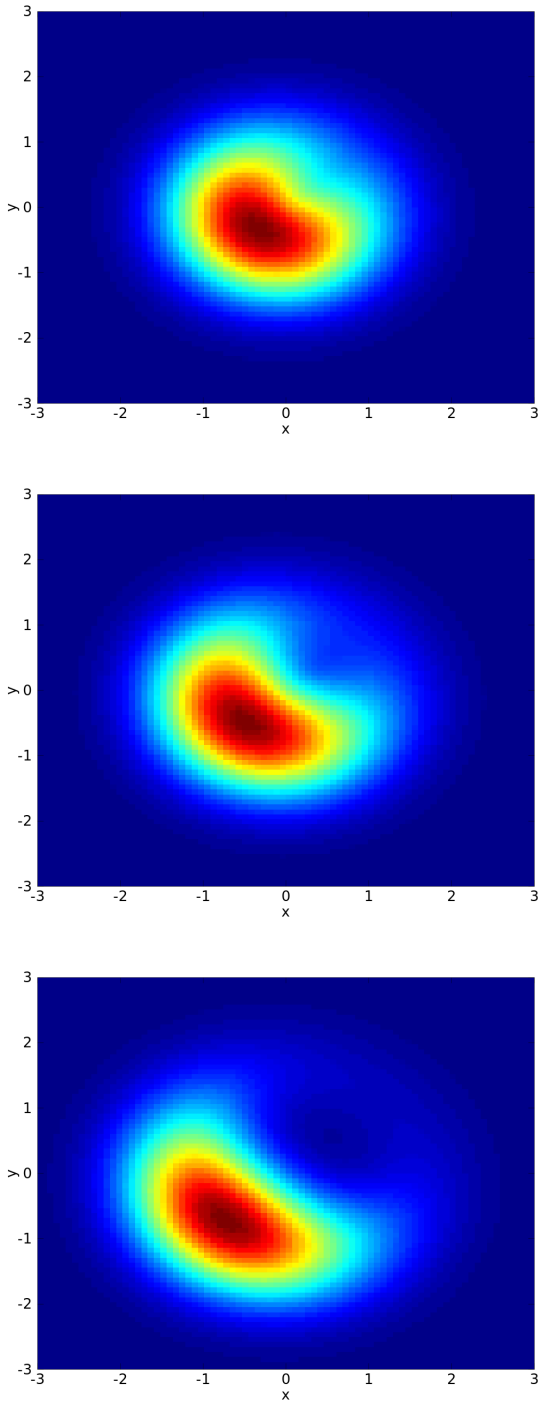

Figure 4.1: The relative probability distribution for two particles in a quantum dot, using trial wave function (4.2), with one of the particles held fixed at an angle $\theta = \pi/4$ for $\lambda = 1.0$, 2.0 and 5.0 (beginning from the top).

Ψ_T	$\langle E/\hbar\omega\rangle$	var$(\langle E/\hbar\omega\rangle)$
$\Psi_T^{1,1}(\overline{x}_1, \overline{x}_2, \overline{y}_1, \overline{y}_2; \alpha, \rho_\alpha, \beta)$	1.3936 ± 0.0001	$(9.4 \pm 0.5) \times 10^{-2}$
$\Psi_T^{1,2}(\overline{x}_1, \overline{x}_2, \overline{y}_1, \overline{y}_2; \alpha, \rho_\alpha, a_2, \beta)$	1.36033 ± 0.00004	$(1.628 \pm 0.006) \times 10^{-2}$
$\Psi_T^{1,3}(\overline{x}_1, \overline{x}_2, \overline{y}_1, \overline{y}_2; \alpha, \rho_\alpha, a_1, a_2, \beta)$	1.35891 ± 0.00003	$(1.39 \pm 0.02) \times 10^{-2}$
Diagonalization [4]	1.3	

Table 4.1: The energy and variance for two particles in one ring with $\rho_0 = 1.8367$ and $\lambda = 1.089$.

$$\Psi_T^{1,1}(\overline{x}_1, \overline{x}_2, \overline{y}_1, \overline{y}_2; \alpha, \rho_\alpha, \beta) = f_T^{1,1}(\rho_1; \alpha, \rho_\alpha) f_T^{1,1}(\rho_2; \alpha, \rho_\alpha) e^{\frac{\lambda\rho_{12}}{1+\beta\rho_{12}}} = e^{-\left((\rho_1-\rho_\alpha)^2+(\rho_2-\rho_\alpha)^2\right)\alpha} e^{\frac{\lambda\sqrt{(\overline{x}_1-\overline{x}_2)^2+(\overline{y}_1-\overline{y}_2)^2}}{1+\beta\sqrt{(\overline{x}_1-\overline{x}_2)^2+(\overline{y}_1-\overline{y}_2)^2}}}. \tag{4.10}$$

Two other trial wave functions were also tested,

$$\Psi_T^{1,2}(\overline{x}_1, \overline{x}_2, \overline{y}_1, \overline{y}_2; \alpha, \rho_\alpha, a_2, \beta) = f_T^{1,4}(\rho_1; \alpha, \rho_\alpha, a_2) f_T^{1,4}(\rho_2; \alpha, \rho_\alpha, a_2) e^{\frac{\lambda\rho_{12}}{1+\beta\rho_{12}}}, \tag{4.11}$$

and

$$\Psi_T^{1,3}(\overline{x}_1, \overline{x}_2, \overline{y}_1, \overline{y}_2; \alpha, \rho_\alpha, a_1, a_2, \beta) = f_T^{1,5}(\rho_1; \alpha, \rho_\alpha, a_1, a_2) f_T^{1,5}(\rho_2; \alpha, \rho_\alpha, a_1, a_2) e^{\frac{\lambda\rho_{12}}{1+\beta\rho_{12}}}. \tag{4.12}$$

The walkers were initially placed between $\rho_0 - 2.5$ and $\rho_0 + 2.5$ in the x- and y-direction. The simulations were performed with 60 000 iterations, of which the 4000 first were removed, using 400 walkers.

Waltersson *et al.* [4] used expansion of the Hamiltonian in B-splines and exact diagonalization for two particles in a quantum ring, with $r_0 = 2.0a_B$, $\hbar\omega = 10$meV, $\epsilon_r = 12.4$ and $m^* = 0.067$. The result for the energy for the singlet state they obtained (read off from a figure) was about $1.3\hbar\omega$. Table 4.1 shows the energy and the variance using trial wave functions (4.10), (4.11) and (4.12) using the same parameters. In scaled units, these parameters correspond to $\rho_0 = 1.8367$ and $\lambda = 1.089$. As in the one particle case, the trial wave functions with a ρ^2 term gave the lowest variance and the lowest energy. Even with trial wave function (4.12), the variance is quite high and the result for the energy is a bit higher than the value obtained by Waltersson *et al.*. Trial wave function (4.12) is used in the rest of this section when $\rho_0 \leq 2$.

Figure 4.2 shows the relative probability distribution calculated from equation (4.9). For $\lambda = 0$ (no interaction) the probability distribution has the same shape as in figure 3.3.

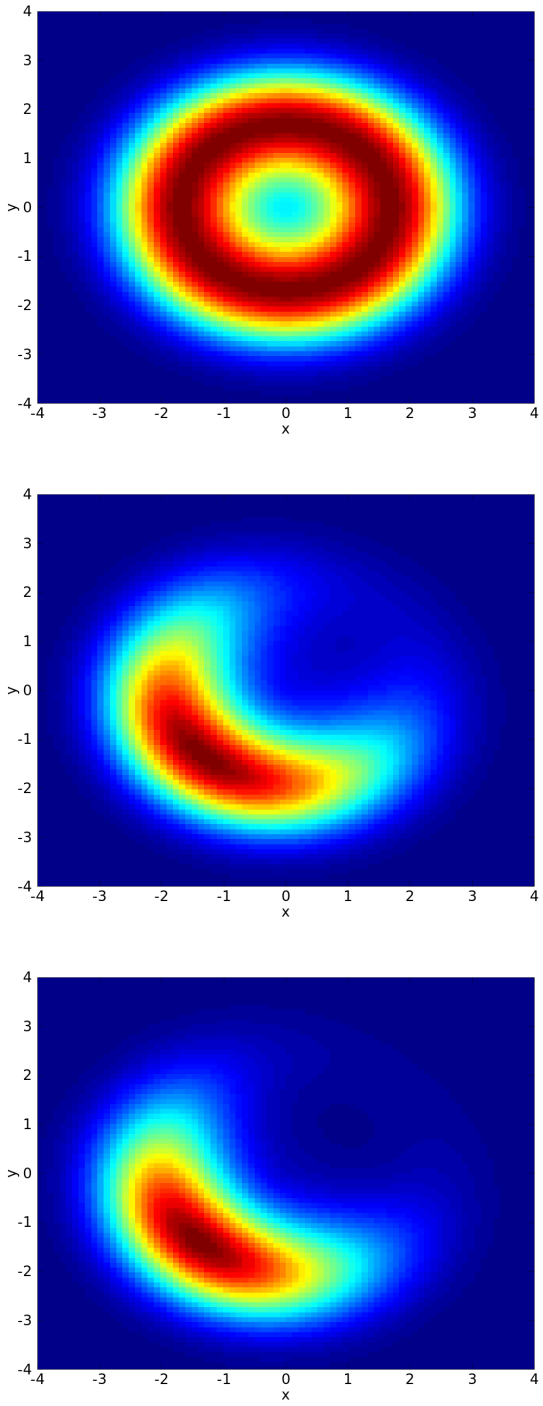

Figure 4.2: The relative probability distribution for a system with two particles in one ring with $\rho_0 = 2.0$, using trial wave function (4.10) for $\lambda = 0.0$, 1.0 and 2.0 (beginning from the top). The position of one of the particles is held fixed at an angle $\theta = \pi/4$.

Figure 4.3 shows the relative probability distribution calculated form equation (4.9) with $\rho_0 = 3.0$. The potential for $\lambda = 0$ now has a true ring shape. The probability distribution is more ring-shaped than when $\rho_0 = 2.0$ for $\lambda = 1$. When the radius is larger the particles can lie further away from each other and the particles will therefore affect each other less. This is also seen in figure 4.4, which shows the energy as a function of λ for a dot and rings with radius 2.0 and 3.0. The smaller the radius, the faster the energy grows with an increasing λ.

The variance increases as λ increases, see figure 4.5. The smaller the radius is, the more the variance increases. The trial wave functions used do thus not describe the system well when the relative importance of the electron-electron interaction is large.

The probability distribution of one of the particles independent of were the other particle is was calculated from

$$P(\rho_1) = \int_{-\infty}^{\infty} |\Psi(\rho_1, \rho_2)|^2 \mathrm{d}\rho_2. \tag{4.13}$$

Figure 4.6 shows the probability distribution, calculated from equation (4.13), using trial wave function (4.12) with $\rho_0 = 2.0$ for six different values of λ. As the values of λ increases, the probability distribution is shifted outwards. When the probability distribution lies further away from the origin, the particles can be further apart.

Figure 4.7 shows the energy as a function of the radius of the ring. As in the one particle case, figure 3.6, the energy initially drops quickly. For large radii the energy goes towards 1.0, which is twice the energy of a particle in a one dimensional harmonic oscillator. The difference between the one and two particle case is that for two particles the minimum is at infinity, wereas for one particle the minimum is around $\rho_0 = 1.5$. For two particles, the larger the ring is, the further away from each of the particles can be, which explains the decrease in the energy.

The variance as a function of the radius of the ring is shown in figure 4.8. The variance is larger for the two particle system than for the one particle system, figure 3.5. As in the one particle case, the variance initially increases to a maximum around 2 and then decreases quickly for large radii. The trial wave functions used gives the best results when the system is, or is close to, a two dimensional harmonic oscillator and when the system is similar to a one dimensional harmonic oscillator.

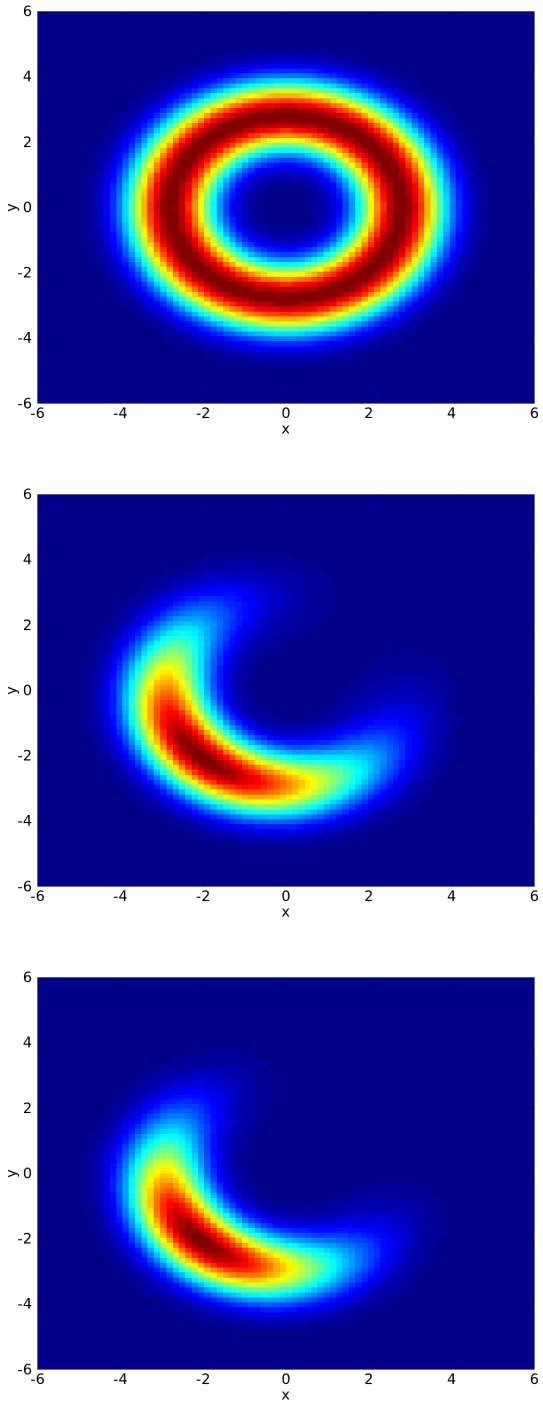

Figure 4.3: The relative probability distribution for a system with two particles in one ring with $\rho_0 = 3.0$, using trial wave function (4.10) for $\lambda = 0.0$, 1.0 and 2.0 (beginning from the top). The position of one of the particles is held fixed at an angle $\theta = \pi/4$.

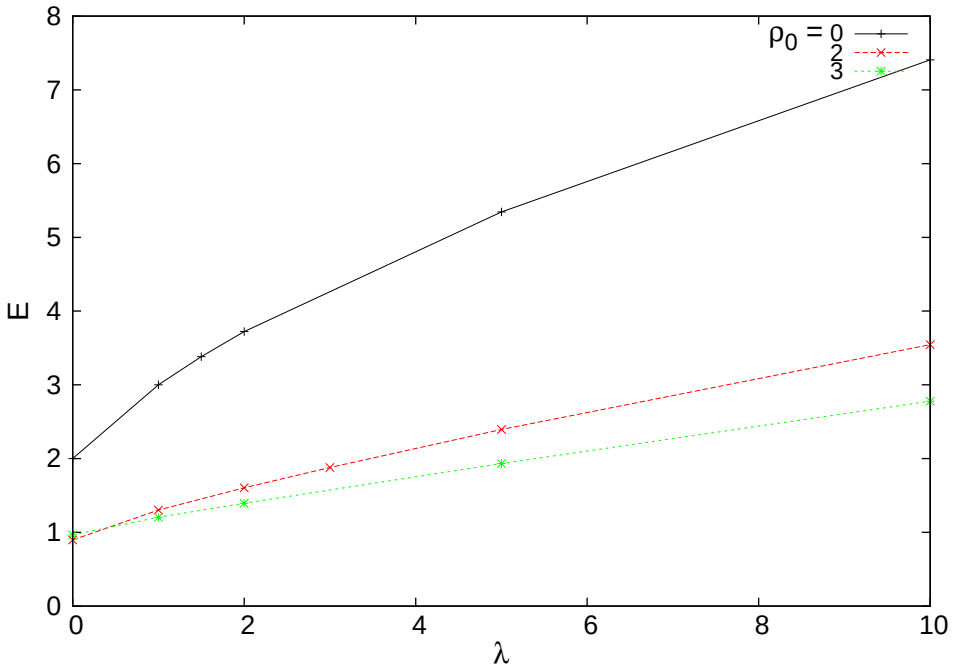

Figure 4.4: The energies as functions of λ for a quantum dot and rings with radius 2.0 and 3.0. The energy is in units of $\hbar\omega$.

4.3 Two particles in two concentric rings

The final system to be studied was two particles in two concentric rings. Equation (3.15) were used for the single particle terms in the trial wave function,

$$\Psi_T^2(\overline{x}_1,\overline{x}_2,\overline{y}_1,\overline{y}_2;\alpha_1,\alpha_2,\rho_{\alpha_1},\rho_{\alpha_2},c,\beta) = f_T^{2,2}(\rho_1;\alpha_1,\alpha_2,\rho_{\alpha_1},\rho_{\alpha_2},c) f_T^{2,2}(\rho_2;\alpha_1,\alpha_2,\rho_{\alpha_1},\rho_{\alpha_2},c) e^{\frac{\lambda\rho_{12}}{1+\beta\rho_{12}}} =$$

$$\left(e^{-\left(\rho_1-\rho_{\alpha_1}\right)^2\alpha_1} + ce^{-\left(\rho_1-\rho_{\alpha_2}\right)^2\alpha_2}\right)\left(e^{-\left(\rho_2-\rho_{\alpha_1}\right)^2\alpha_1} + ce^{-\left(\rho_2-\rho_{\alpha_2}\right)^2\alpha_2}\right) e^{\frac{\lambda\sqrt{(\overline{x}_1-\overline{x}_2)^2+(\overline{y}_1-\overline{y}_2)^2}}{1+\beta\sqrt{(\overline{x}_1-\overline{x}_2)^2+(\overline{y}_1-\overline{y}_2)^2}}} \tag{4.14}$$

The walkers were initially placed between $\rho_{0,1} - 2.5$ and $\rho_{0,2} + 2.5$ in the x- and y-direction. The simulations using the same number of iterations as in the one ring case.

Figure 4.9 shows the probability distribution for three different values of the outer radius with $\rho_{0,1} = 3.0$, $\lambda = 1.0$ and $\omega_1 = \omega_2 = 1.0$. As the outer radius gets larger, the probability for the particles to be in the outer ring increases. This is the opposite of the one particle case, see figure 3.11, were the probability of being in the outer ring decreased as the value of $\rho_{0,2}$

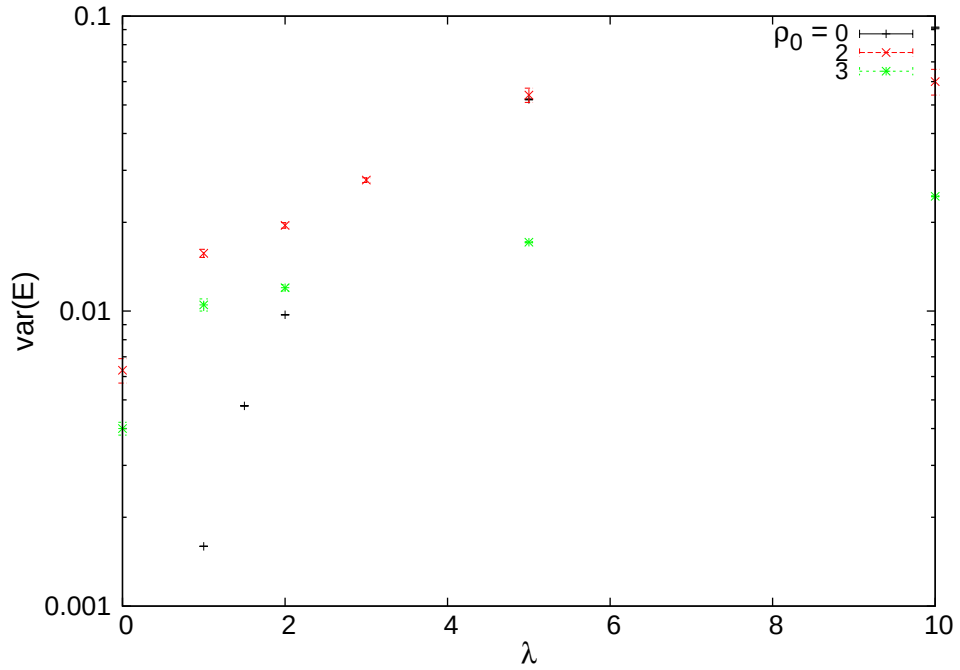

Figure 4.5: The variance for different values of λ for a quantum dot and rings with radius 2.0 and 3.0. The energy is in units of $\hbar\omega$.

$\rho_{0,2}$	$\langle E/\hbar\omega_1 \rangle$	var$(\langle E/\hbar\omega_1 \rangle)$	$\langle \rho_{12} \rangle$	$P_{\rho<\rho_c}$
6.0	0.9476 ± 0.0001	$(1.321 \pm 0.005) \times 10^{-2}$	8.440 ± 0.003	0.37738 ± 0.00009
7.0	1.066370 ± 0.00008	$(7.13 \pm 0.05) \times 10^{-3}$	11.103 ± 0.004	0.14526 ± 0.00009
8.0	1.07678 ± 0.00006	$(4.91 \pm 0.02) \times 10^{-3}$	14.157 ± 0.008	0.00357 ± 0.00007

Table 4.2: The energy and variance for two particles in two rings, with $\lambda = 1.0$, $\rho_{0,1} = 3.0$ and $\omega_1 = \omega_2 = 1.0$.

got larger. For two particles in one ring the energy decreases as the radius increases, see figure 4.7. For one particle in one ring on the other hand, the energy increases after after the minimum around 1.5, see figure 3.6. So, for one particle, when $\rho_{0,1}$ is larger than 2, the inner ring has the lowest energy and therefore the particle has a larger probability of being in the inner ring. In the two particle case the outer ring has the lowest energy and therefore there is a larger probability for a particle to be in the outer ring. This is since the particles can be further away from each other in the outer ring. As in the one particle case, the energy for two particles increases as the outer radius increases, since the potential gets smaller, see figure 3.10. When $\rho_{0,2} = 8.0$ the energy is about the same as for two particles in a ring with radius 8.0.

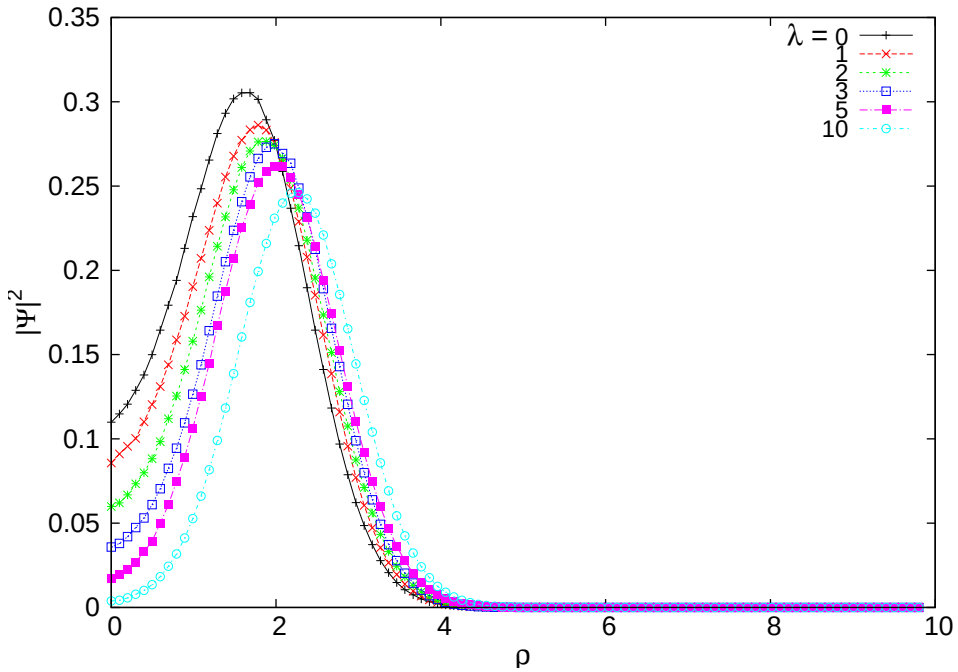

Figure 4.6: The probability distribution using trial wave function (4.12) for five different values of λ for $\rho_0 = 2.0$.

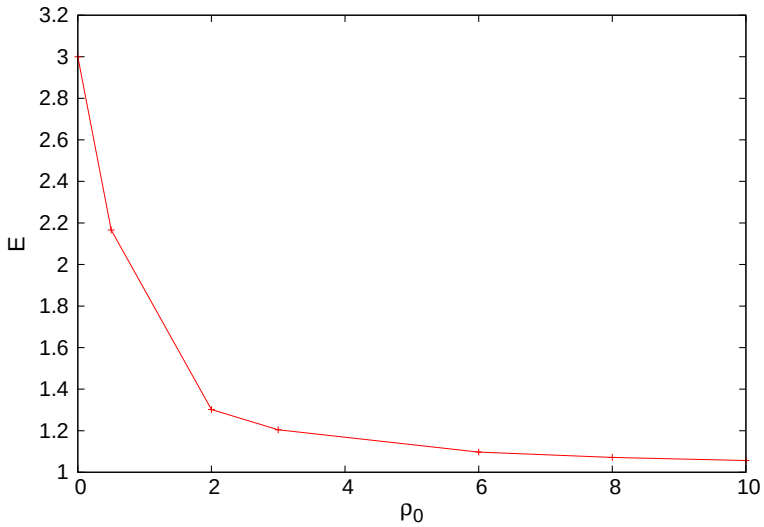

Figure 4.7: The energy as a function of the radius of the ring for two particles with $\lambda = 1.0$. The energy is in units of $\hbar\omega$.

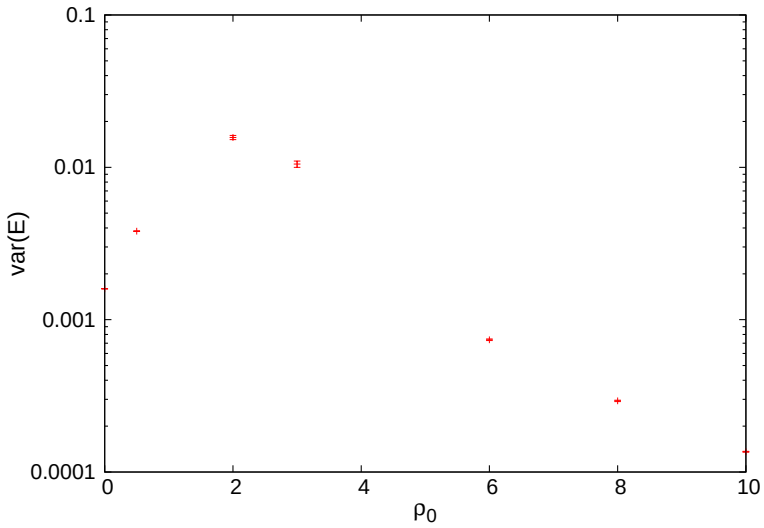

Figure 4.8: The variance for different radius of the ring for two particles with $\lambda = 1.0$. The energy is in units of $\hbar\omega$.

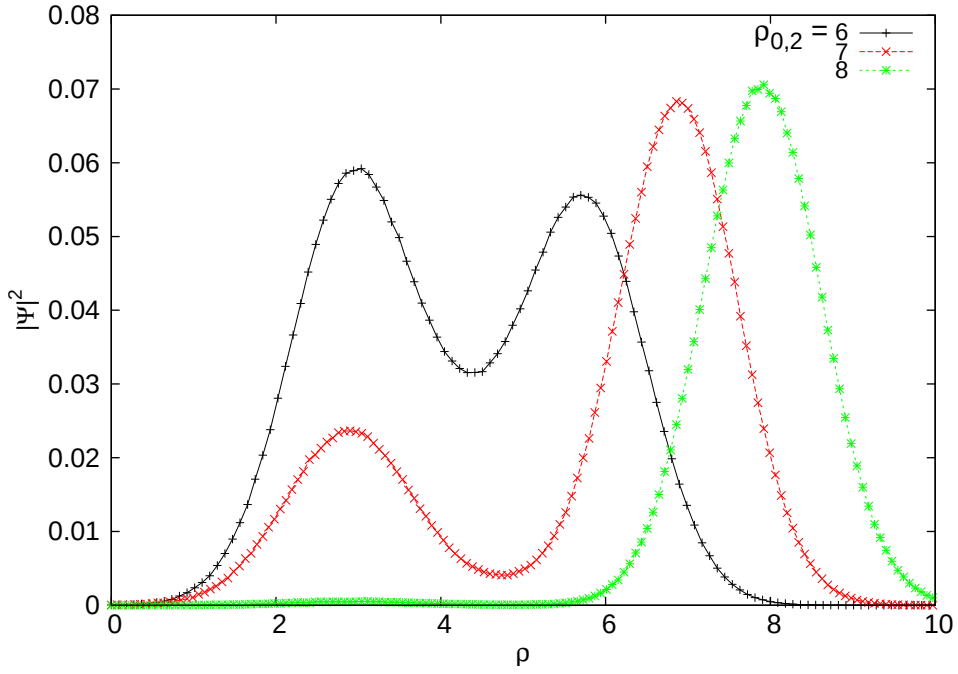

Figure 4.9: The probability distribution using equation (4.14) for three different values of $\rho_{0,2}$ with $\rho_{0,1} = 3.0$, $\lambda = 1.0$ and $\omega_1 = \omega_2 = 1.0$.

λ	$\langle E/\hbar\omega_1 \rangle$	var$(\langle E/\hbar\omega_1 \rangle)$	$\langle \rho_{12} \rangle$	$P_{\rho<\rho_c}$
0.0	0.96553 ± 0.00005	$(5.0 \pm 0.3) \times 10^{-3}$	3.923 ± 0.003	0.99970 ± 0.00009
0.05	0.98304 ± 0.00005	$(2.92 \pm 0.01) \times 10^{-3}$	6.13 ± 0.02	0.72976 ± 0.00005
0.1	0.99550 ± 0.00006	$(2.26 \pm 0.02) \times 10^{-3}$	8.23 ± 0.02	0.48258 ± 0.00006
0.25	1.01739 ± 0.00007	$(3.1 \pm 0.2) \times 10^{-3}$	10.32 ± 0.02	0.28183 ± 0.00008
1.0	1.07678 ± 0.00006	$(4.91 \pm 0.02) \times 10^{-3}$	14.157 ± 0.008	0.00357 ± 0.00007

Table 4.3: The energy and variance for two particles in two rings, $\rho_{0,1} = 3.0$, $\rho_{0,2} = 8.0$ and $\omega_1 = \omega_2 = 1.0$

Figure 4.10 shows the probability distribution for four different values of λ with $\rho_{0,1} = 3.0$, $\rho_{0,2} = 8.0$ and $\omega_1 = \omega_2 = 1.0$. For $\lambda = 0.0$ the probability of finding the particle in the inner ring is close to 1, while for $\lambda = 1.0$ the probability is close to 0, see table 4.3. The probability of being in the outer ring changes rapidly as λ increases form zero.

To check the program, simulations were done for parameters were the result had previously been obtained with quantum Monte Carlo. Colletti *et al.* [6] used variational Monte Carlo (VMC) and diffusion Monte Carlo (DMC) for two electrons in two concentric rings. The parameters used were $r_{0,1} = 60$nm, $r_{0,2} = 90$nm, $\hbar\omega_1 = 35$meV, $m^* = 0.067m_e$, $\epsilon_r = 12.4$ and six different values of $\hbar\omega_2$ ranging from 30 to 40 meV.

In reduced units the parameters are $\rho_{0,1} = 10.5256$, $\rho_{0,2} = 15.7884$ and $\lambda = 0.5802$, and equation (2.16). The result is shown in table 4.4 and 4.5. When $\hbar\omega_2 >= 35.62$ the energies are slightly higher than the values obtained by [6]. When $\hbar\omega_2 <= 35.15$, the energies are lower than the VMC values and higher than the DMC values obtained by [6]. The variance is quite low for all values of $\hbar\omega_2$.

Figure 4.11 shows the probability distribution using the six different values of $\hbar\omega_2$. When $\hbar\omega_2 >= 35.62$ the particles are mostly in the inner ring and when $\hbar\omega_2 <= 35.15$ the particles are mostly in the outer ring. The crossover happens for a value of $\hbar\omega_2$ which is a bit higher than the result found by [6] and it also happens more slowly. Colletti *et al.* found that the particles went from being mostly in the inner ring to mostly in the outer ring between $\hbar\omega_2 = 35.15$ and $\hbar\omega_2 = 35.14$. This is probably an effect of the trial wave function used. Colletti *et al.* used varied only the parameters in the Jastrow function and used the single-particle result for the parameters in the single-particle part.

Figure 4.12 shows the relative probability distribution with one of the particles held fixed at an angel $\theta = \pi/4$. In the first plot, $\hbar\omega_2 = 35.62$, most of the probability distribution lies in the inner ring. With $\hbar\omega_2 = 35.30$, the

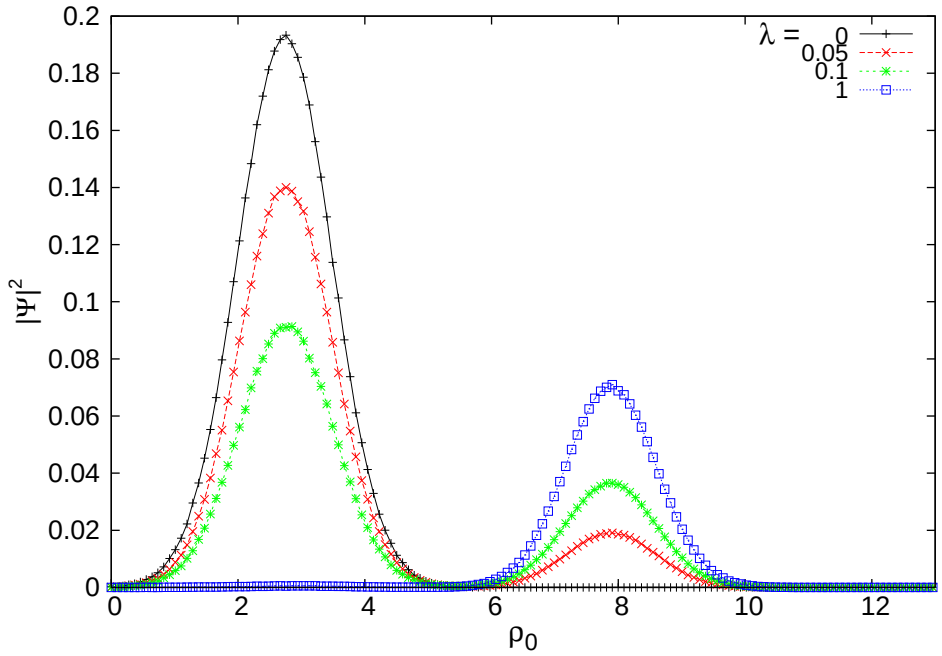

Figure 4.10: The probability distribution using trial wave function (4.14) for different values of λ with $\rho_{0,1} = 3.0$, $\rho_{0,2} = 8.0$ and $\omega_1 = \omega_2 = 1.0$.

second plot, the probability for the particles to be in the inner ring is 0.44. In the last plot, $\hbar\omega_2 = 35.15$, the probability distribution is almost entirely in the outer ring. When the probability to be in the inner ring decreases the probability distribution in the inner ring will lie further away from the other particle.

$\hbar\omega_2$(meV)	$E_{DMC}/\hbar\omega_1$[6]	$E_{VMC}/\hbar\omega_1$[6]	$\langle E/\hbar\omega_1\rangle$
40.0	1.0314	1.0351	1.03565 ± 0.00002
37.0	1.0311	1.0341	1.03553 ± 0.00002
35.62	1.0310	1.0322	1.03362 ± 0.00002
35.15	1.0202	1.0322	1.02560 ± 0.00002
35.14	1.0239	1.0268	1.02535 ± 0.00002
30.0	0.87767	0.88011	0.87946 ± 0.00001

Table 4.4: The energy for two particles in two rings, $r_{0,1} = 60$nm, $r_{0,2} = 90$nm, $\hbar\omega_1 = 35$meV, $m^* = 0.067m_e$ and $\epsilon_r = 12.4$ compared with the energies obtained by [6].

$\hbar\omega_2$(meV)	var($\langle E/\hbar\omega_1\rangle$)	$\langle\rho_{12}\rangle$	$P_{\rho<\rho_c}$
40.0	$(2.166 \pm 0.005) \times 10^{-3}$	18.294 ± 0.006	0.99981 ± 0.00002
37.0	$(2.226 \pm 0.004) \times 10^{-3}$	18.317 ± 0.005	0.99954 ± 0.00002
35.62	$(2.031 \pm 0.006) \times 10^{-3}$	20.20 ± 0.01	0.79600 ± 0.00002
35.15	$(1.415 \pm 0.004) \times 10^{-3}$	27.14 ± 0.01	$(8.72617 \pm 0.00002) \times 10^{-2}$
35.14	$(1.436 \pm 0.004) \times 10^{-3}$	27.12 ± 0.01	$(8.96281 \pm 0.00002) \times 10^{-2}$
30.0	$(1.020 \pm 0.002) \times 10^{-3}$	27.95 ± 0.01	$(2.066267 \pm 0.00001) \times 10^{-3}$

Table 4.5: The variance, the expectation value of the distance between the particles and the probability for the particles to be in the inner ring for two particles in two rings, $r_{0,1} = 60$nm, $r_{0,2} = 90$nm, $\hbar\omega_1 = 35$meV and the effective mass and dielectric constant of GaAs.

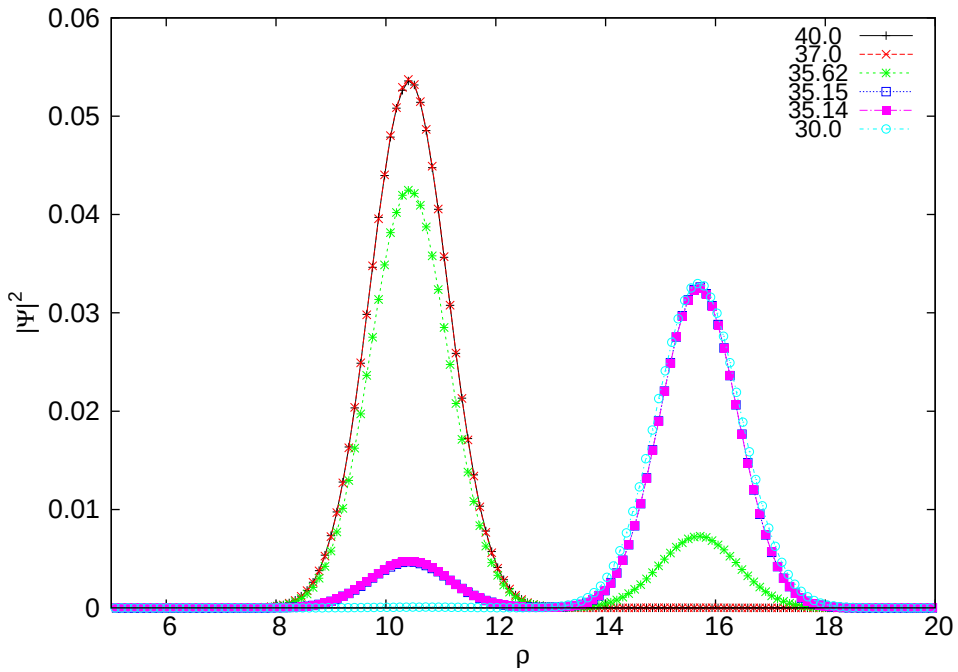

Figure 4.11: The probability distribution for different values of $\hbar\omega_2$ (in meV) with $\hbar\omega_1 = 35$meV, $\rho_{0,1} = 10.5256$, $\rho_{0,2} = 15.7884$ and $\lambda = 0.5802$.

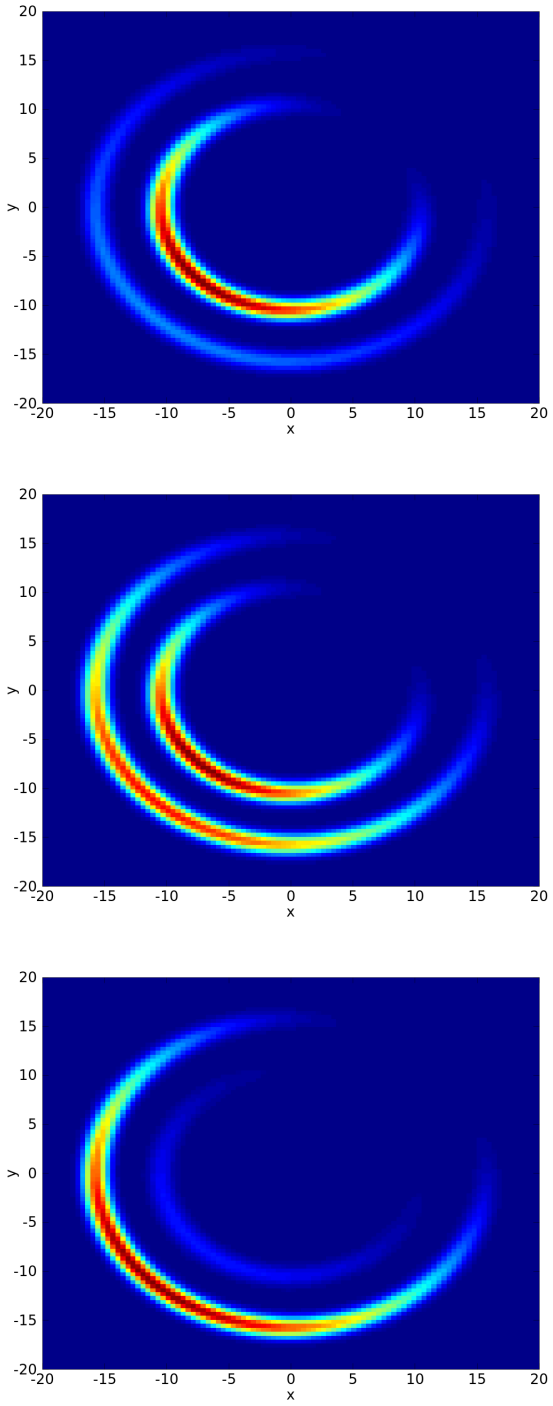

Figure 4.12: The relative probability distribution for a system with two particles in two rings with $\hbar\omega_1 = 35\text{meV}$, $\rho_{0,1} = 10.5256$, $\rho_{0,2} = 15.7884$ and $\lambda = 0.5802$ using $\hbar\omega_2 = 35.62\text{meV}$, 35.30meV and 35.15meV (beginning form the top). The position of one of the particles is held fixed at an angle $\theta = \pi/4$.

Chapter 5

Conclusions and outlook

In this thesis the ground state energy has been calculated for one and two particles in a quantum dot, one ring and two concentric rings using the variational Monte Carlo method.

For one particle in one ring good agreement were found for all five radii tested ($\rho_0 = 0.5$, 2, 3, 10 and 50) when comparing with an existing routine which used expansion of the Hamiltonian in a B-Spline basis and exact diagonalization. The effect of the radius of the ring on the energy and the variance were also studied. As the radius increased from 0, the energy was found to initially decrease to a minimum around 1.5, after which it slowly increased towards the energy of a one dimensional harmonic oscillator. The variance were found to be the largest for radii between 1 and 3 and that the trial wave functions used therefore described those systems least well. For small radii, a polynomial with a quadratic term were needed in the trial wave function to get good results.

Good agreement with the results obtained with diagonalization was also found for one particle in two concentric rings. As the radius of the outer ring increased with the radius of the inner ring held fixed, the probability for the particle to be in the inner ring was found to increase.

The energy obtained for two particles in a quantum dot agreed well with the exact result.

For two particles in a ring with radius $\rho_0 = 1.8367$ the energy was a bit higher than the result obtained by Waltersson *et al.*. As in the case of one particle in one ring, the variance the highest and the result the least accurate when the radius was around 2 for two particles. A better trial wave function for the single particle part would give a better result for two particles in a small ring, at the expense of introducing more variational parameters.

The energy was found to decrease as the radius increased for two particles in one ring. For large radii the energy approached twice the value of one

particle in a one dimensional harmonic oscillator.

For two particles in two concentric rings, the program was checked by comparing with results obtained by Colletti *et al.* [6]. Good agreement was found between the energies. The crossover between the situation when the particles are mostly in the inner ring to the situation when the particles are mostly in the outer ring occurred between $\hbar\omega_2 = 35.15$meV and $\hbar\omega_2 = 35.62$meV. This is slightly higher than the value obtained by [6] and the crossover also happened more slowly.

The probability to be in the inner ring decreased as the outer radius increased, the opposite to the one particle case. For one particle in one ring, the energy as a function of the radius had a minimum around 1.5. When the distance between the rings is large, the particle will mostly lie in the ring closest to the minimum.

The maximum number of variational parameters used was 6. If one would use more parameters a more effective minimization routine is probably needed. Using the gradient in the minimization reduces the number of line minimization needed. Then a few more parameters could be used before needing to use parallellization.

One way one could try to improve the trial wave functions is to include more polynomial terms. If many parameters are needed, around 30 or more, it might be better to use B-splines than global trial wave functions. Then the coefficients are the parameters to be optimized.

One way to continue the studies of quantum rings would be to add one more particle. For two or more particles the Pauli principle needs to be respected, that is the wave function should be antisymmetric under exchange of any two particles. For three particles the need to respect the Pauli principle requires an explicitly antisymmetrized trial wave function. For N particles the Slater-Jastrow function [10] can be written

$$\Psi_T^N(x_1, ..., x_N) = \Psi_{AS}(x_1, ..., x_N)\exp\left[\frac{1}{2}\sum_{i,j}^{N}\Phi(r_{ij})\right]. \tag{5.1}$$

The single particle part is given by the Slater determinant $\Psi_{AS}(x_1, ..., x_N)$, which is an antisymmetric product of the single particle wave functions. The other part is the Jastrow function which is symmetric. Thus the total wave function is antisymmetric. The Slater determinant was not used for the two particle case since the particles were assumed to be in a singlet state, that is the spin wave function was assumed to be antisymmetric. The spatial part is in that case symmetric.

Chapter 6

Appendix

To compute the local energy, equation (2.18), one need to compute $H\Psi_T$. The Hamiltonian for two particles in Cartesian coordinates is

$$H = \hbar\omega\left(\left(\sum_{i=1}^{2} -\frac{1}{2}\left(\frac{\partial^2}{\partial\overline{x}_i^2} + \frac{\partial^2}{\partial\overline{y}_i^2}\right) + \frac{V(\overline{x},\overline{y})}{\hbar\omega}\right) + \frac{\lambda}{\rho_{12}}\right). \tag{6.1}$$

The Hamiltonian contains the ∇^2 operator,

$$\nabla^2 = \frac{\partial^2}{\partial\overline{x}^2} + \frac{\partial^2}{\partial\overline{y}^2} = \frac{1}{r}\frac{\partial}{\partial r} + \frac{\partial^2}{\partial r^2} + \frac{1}{r^2}\frac{\partial^2}{\partial\theta^2}. \tag{6.2}$$

Since the trial wave functions used for the two particle systems are written partly in cylindrical coordinates and partly in Cartesian coordinates the chain rule is needed.

$$\frac{\partial}{\partial x} = \frac{\partial r}{\partial x}\frac{\partial}{\partial r} + \frac{\partial\theta}{\partial x}\frac{\partial}{\partial\theta} = \frac{x}{r}\frac{\partial}{\partial r} - \frac{y}{r}\frac{\partial}{\partial\theta}, \tag{6.3}$$

$$\frac{\partial}{\partial y} = \frac{\partial r}{\partial y}\frac{\partial}{\partial r} + \frac{\partial\theta}{\partial y}\frac{\partial}{\partial\theta} = \frac{y}{r}\frac{\partial}{\partial r} + \frac{x}{r}\frac{\partial}{\partial\theta}. \tag{6.4}$$

Because of spherical symmetry the terms including θ are not needed.

We need to calculate $-\left(\nabla_1^2 + \nabla_2^2\right)\Psi_T/2$. Taking two particles in one ring and trial wave function (4.10) as an example (set $\rho_\alpha = 0$ for a quantum dot), and looking at the first index

$$-\frac{1}{2}\nabla_1^2\Psi_T = -\frac{1}{2}\left(\left(\frac{1}{\rho}\frac{\partial}{\partial\rho} + \frac{\partial^2}{\partial\rho^2}\right)e^{-\alpha_1(\rho_1-\rho_{\alpha_1})^2}\right)\times e^{-\alpha_1(\rho_2-\rho_{\alpha_1})^2}\times e^{\frac{\lambda\sqrt{(\overline{x}_1-\overline{x}_2)^2+(\overline{y}_1-\overline{y}_2)^2}}{1+\beta\sqrt{(\overline{x}_1-\overline{x}_2)^2+(\overline{y}_1-\overline{y}_2)^2}}} \tag{6.5}$$

$$-\frac{1}{2}e^{-\alpha_1(\rho_1-\rho_{\alpha_1})^2}\times e^{-\alpha_1(\rho_2-\rho_{\alpha_1})^2}\times\left(\frac{\partial^2}{\partial\overline{x}_1^2} + \frac{\partial^2}{\partial\overline{y}_1^2}\right)e^{\frac{\lambda\sqrt{(\overline{x}_1-\overline{x}_2)^2+(\overline{y}_1-\overline{y}_2)^2}}{1+\beta\sqrt{(\overline{x}_1-\overline{x}_2)^2+(\overline{y}_1-\overline{y}_2)^2}}} \tag{6.6}$$

$$-\left(\frac{\rho_1}{\overline{x}_1}\frac{\partial}{\partial\rho_1}e^{-\alpha_1(\rho_1-\rho_{\alpha_1})^2}\right)\times e^{-\alpha_1(\rho_2-\rho_{\alpha_1})^2}\times\frac{\partial}{\partial\overline{x}_1}e^{\frac{\lambda\sqrt{(\overline{x}_1-\overline{x}_2)^2+(\overline{y}_1-\overline{y}_2)^2}}{1+\beta\sqrt{(\overline{x}_1-\overline{x}_2)^2+(\overline{y}_1-\overline{y}_2)^2}}} \quad (6.7)$$

$$-\left(\frac{\rho_1}{\overline{y}_1}\frac{\partial}{\partial\rho_1}e^{-\alpha_1(\rho_1-\rho_{\alpha_1})^2}\right)\times e^{-\alpha_1(\rho_2-\rho_{\alpha_1})^2}\times\frac{\partial}{\partial\overline{y}_1}e^{\frac{\lambda\sqrt{(\overline{x}_1-\overline{x}_2)^2+(\overline{y}_1-\overline{y}_2)^2}}{1+\beta\sqrt{(\overline{x}_1-\overline{x}_2)^2+(\overline{y}_1-\overline{y}_2)^2}}} \quad (6.8)$$

The term (6.5) gives the contribution

$$\alpha_1-2\alpha_1^2\left(\rho_1-\rho_{\alpha_1}\right)^2+\frac{1}{\rho_1}\alpha_1\left(\rho_1-\rho_{\alpha_1}\right). \quad (6.9)$$

The contribution to the local energy from term (6.6) is

$$\frac{1}{2}\left(\frac{3\beta\lambda}{\left(1+\beta\rho_{12}\right)^3}+\frac{\lambda}{\left(1+\beta\rho_{12}\right)^3\rho_{12}}-\frac{2\lambda}{\left(1+\beta\rho_{12}\right)^2\rho_{12}}-\frac{\lambda^2}{\left(1+\beta\rho_{12}\right)^4}\right)=$$

$$\frac{1}{2}\left(\frac{\beta\lambda}{\left(1+\beta\rho_{12}\right)^3}-\frac{\lambda}{\left(1+\beta\rho_{12}\right)^3\rho_{12}}-\frac{\lambda^2}{\left(1+\beta\rho_{12}\right)^4}\right) \quad (6.10)$$

The term (6.7) gives the contribution

$$\frac{\overline{x}_1}{\rho_1}2\alpha_1\left(\rho_1-\rho_{\alpha_1}\right)\frac{\lambda\left(\overline{x}_1-\overline{x}_2\right)}{1+\beta\sqrt{(\overline{y}_1-\overline{y}_2)^2+(\overline{y}_1-\overline{y}_2)^2}}\times$$

$$\left(\frac{1}{\sqrt{(\overline{x}_1-\overline{x}_2)^2+(\overline{y}_1-\overline{y}_2)^2}}-\frac{\beta}{1+\beta\sqrt{(\overline{x}_1-\overline{x}_2)^2+(\overline{y}_1-\overline{y}_2)^2}}\right)=$$

$$\frac{\overline{x}_1}{\rho_1}\frac{\lambda\left(\overline{x}_1-\overline{x}_2\right)}{\left(1+\beta\rho_{12}\right)^2}\frac{2\alpha_1\left(\rho_1-\rho_{\alpha_1}\right)}{\rho_{12}} \quad (6.11)$$

The term (6.8) gives the same contribution as equation (6.11) but with $\overline{x}_1\rightarrow\overline{y}_1$ and $\overline{x}_2\rightarrow\overline{y}_2$.

References

1. A. Fuhrer, S. Lüscher, T. Ihn, T. Heinzel, K. Ensslin, W. Wegscheider and M. Bichler, Microelectron eng. **63**, 47-52 (2002).

2. A. Lorke, R. J. Luyken, A. O. Govorov, J. P. Kotthaus, J. M. Garcia and P. M. Petroff. Phys. Rev. Lett. **84**, 2223 (2000).

3. A. Kumar, S. E. Laux and F. Stern. Phys. Rev. B **42**, 5166-5175 (1990)

4. E. Waltersson, E. Lindroth, I. Pilskog and J. P. Hansen. Phys. Rev. B **79**, 115318 (2009).

5. S. Viefers, P. Koskinen, P. Singha Deo and M. Manninen. Physica E **21**, 1-25 (2004)

6. L. Colletti, F. Malet, M. Pi and F. Pederiva. Phys. Rev. B **79**, 125315 (2009).

7. Jos M. Thijssen. *Computational Physics*. Cambridge University Press 2013.

8. N. Metropolis, A. W. Rosenbluth, M. N. Rosenbluth, A. H. Teller and E. Teller. J. Chem. Phys. **21**, 1087 (1953).

9. William H. Press, Saul A. Teukolsky, William T. Vetterling and William B. Flannery. *Numerical Recipes in C*. Cambridge University Press 2002.

10. R. Jastrow. Phys. Rev. **98**, 1479 (1955).

11. E. Räsänen, H. Saarikoski, V. N. Stavrou, A. Harju, M. J. Puska and R. M. Nieminen. Phys. Rev. Lett. **67**, 235307 (2003).

12. M. Taut. J. Phys. A **27**, 1045 (1994)